AD-A069 173 AIR FORCE ENGINEERING AND SERVICES CENTER TYNDALL AF--ETC F/G 13/2
THE AUTOXIDATION OF MONOMETHYLHYDRAZINE VAPOR.(U)
APR 79 D A STONE

UNCLASSIFIED AFESC/ESL-TR-79-10 NL

| OF |
AD A069173

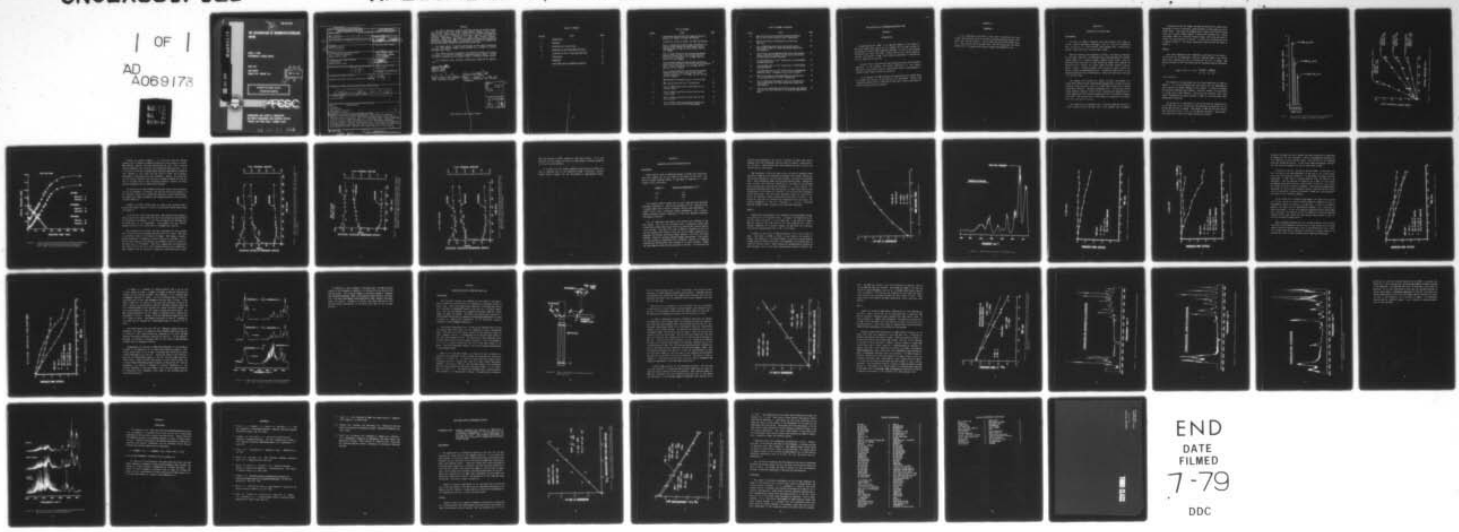

END
DATE FILMED
7-79
DDC

ESL-TR-79-10

THE AUTOXIDATION OF MONOMETHYLHYDRAZINE VAPOR

DANIEL A. STONE
ENVIRONMENTAL SCIENCES BRANCH

APRIL 1979

FINAL REPORT
JANUARY 1978 - JANUARY 1979

APPROVED FOR PUBLIC RELEASE;
DISTRIBUTION UNLIMITED

ENGINEERING AND SERVICES LABORATORY
AIR FORCE ENGINEERING AND SERVICES CENTER
TYNDALL AIR FORCE BASE, FLORIDA 32403

UNCLASSIFIED

SECURITY CLASSIFICATION OF THIS PAGE (When Data Entered)

REPORT DOCUMENTATION PAGE

READ INSTRUCTIONS BEFORE COMPLETING FORM

1. REPORT NUMBER: ESL - TR-79-10

2. GOVT ACCESSION NO.

3. RECIPIENT'S CATALOG NUMBER

4. TITLE (and Subtitle): THE AUTOXIDATION OF MONOMETHYLHYDRAZINE VAPOR.

5. TYPE OF REPORT & PERIOD COVERED: Final Report. Jan 78 - Jan 79

6. PERFORMING ORG. REPORT NUMBER

7. AUTHOR(s): Daniel A. Stone

8. CONTRACT OR GRANT NUMBER(s)

9. PERFORMING ORGANIZATION NAME AND ADDRESS: Det 1 (CEEDO) HQ AFESC/ECC, Tyndall AFB FL 32403

10. PROGRAM ELEMENT, PROJECT, TASK AREA & WORK UNIT NUMBERS: Program Element 62601F, Project 1900

11. CONTROLLING OFFICE NAME AND ADDRESS: HQ AFESC/RDVC, Tyndall AFB FL 32403

12. REPORT DATE: Apr 79

13. NUMBER OF PAGES: 44

14. MONITORING AGENCY NAME & ADDRESS (if different from Controlling Office)

15. SECURITY CLASS. (of this report): UNCLASSIFIED

15a. DECLASSIFICATION/DOWNGRADING SCHEDULE

16. DISTRIBUTION STATEMENT (of this Report)

Approved for public release; distribution unlimited

17. DISTRIBUTION STATEMENT (of the abstract entered in Block 20, if different from Report)

AFESC/ESL-TR-79-10

18. SUPPLEMENTARY NOTES

Available in DDC

19. KEY WORDS (Continue on reverse side if necessary and identify by block number)

MMH
Missile Fuels
Oxidation
Air Pollution
Environmental Simulation
Environmental Quality

20. ABSTRACT (Continue on reverse side if necessary and identify by block number)

Results of experiments simulating atmospheric autoxidation of monomethylhydrazine vapor are presented. MMH partial pressures ranged from a few ppm to a few Torr and all experiments were run at room temperature. Results show that the main products of MMH autoxidation in air are formaldehyde monomethylhydrazone, methane, methanol, nitrogen and water. The reaction rate appears to be heterogeneously controlled with surface activity and surface to volume ratio being important factors. MMH half life ranged from two to seven hours.

DD FORM 1 JAN 73 1473

394 633

UNCLASSIFIED

SECURITY CLASSIFICATION OF THIS PAGE (When Data Entered)

PREFACE

The report documents research performed during the period January 1978 through January 1979 under Program Element 62601F, Project 1900, Subtask 2013. This research was carried out at the CEEDO environmental chemistry laboratory at Tyndall Air Force Base, Florida. The author and principal investigator is Daniel A. Stone, PhD, research chemist. Effective 1 March 1979 CEEDO was inactivated and became the Engineering and Services Laboratory (ESL), a directorate of the Air Force Engineering and Services Center located on Tyndall AFB Florida 32403.

The author wishes to express appreciation for the helpful discussion and mass spectrometric support ably provided by Lt Joseph A. Zirrolli throughout this effort.

This report has been reviewed by the Information Office (OI) and is releasable to the National Technical Information Service (NTIS). At NTIS it will be available to the general public, including foreign nations.

This technical report has been reviewed and is approved for publication.

Daniel A. Stone
DANIEL A. STONE,
Research Chemist

Peter A. Crowley
PETER A. CROWLEY, Maj, USAF, BSC
Chief, Environics Division

Joseph S. Pizzuto
JOSEPH S. PIZZUTO, Col, USAF, BSC
Director, Engineering and Services Laboratory

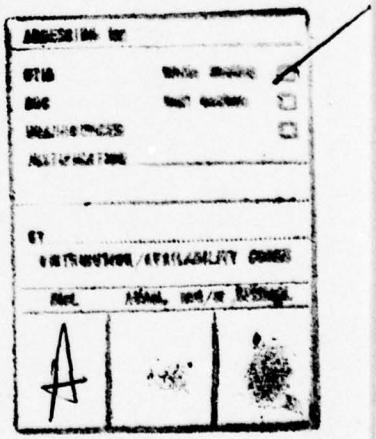

(The reverse of this page is blank)

TABLE OF CONTENTS

LIST OF FIGURES

LIST OF FIGURES (Continued)

THE AUTOXIDATION OF MONOMETHYLHYDRAZINE VAPOR

SECTION I

INTRODUCTION

Monomethylhydrazine (MMH) is an important member of the family of hydrazine based fuels which are an integral part of many current or developing Air Force rocket propulsion systems. In view of the problems associated with spill and vapor releases which occur during handling, storage, and transfer of MMH, this study was undertaken to characterize the air oxidation of this fuel.

Previous work in this area has been reported by Vernot and Co-workers (Reference 1) and Saunders and Larkins (Reference 2). The reseach described in this report seeks to extend these earlier investigations to include a wider range of reaction conditions.

It is essential that MMH oxidation be characterized to a degree which will enable the kinetics of this process to be determined. Further, MMH oxidation products must be identified so that their relative importance or potential hazards may be evaluated.

SECTION II

MATERIALS

In all experiments described in this report, hydrazines were used without further purification as received from Rocky Mountain Arsenal (fuel grade, 98 + percent purity). The nitrogen gas was 99.998 percent pure, the oxygen gas was 99.99 percent pure, and the helium gas was 99.999 percent pure. All gases were from Air Products and Chemicals, Inc.

SECTION III

OXIDATION IN A 300-ML FLASK

EXPERIMENTAL

In order to compare oxidation rates and products with those of earlier, similar experiments (Reference 1 and 3), a series of oxidations were carried out in a 300-ml Pyrex® flask equipped with a Fisher-Porter Teflon® vacuum valve and a silicon rubber septum.

Reaction mixtures were prepared as follows. The bulb was evacuated to less than 5 millitorr (as measured with a Hastings Model VH-3 thermocouple gauge) on a liquid nitrogen trapped vacuum system. Then the desired partial pressures of tank helium and oxygen were admitted as measured with a Wallace and Tiernan Model FA-160230 absolute pressure gauge. Finally, a Unimetrics Model 5050R syringe was used to inject the desired volume of monomethylhydrazine. Mixing and vaporization of the monomethylhydrazine were accomplished by shaking the flask which contained a few Teflon® chips.

Gas samples were analyzed for oxygen, nitrogen, and methane on a Perkin Elmer Model 900 gas chromatograph equipped with a 6-foot by ⅛-inch stainless steel molecular sieve 5-A column (45/60 mesh) and a thermal conductivity detector. Operating parameters were: carrier gas flow 60 cc/min (helium), detector current 175 mA, injection port temperature 50°C, column temperature 70°C, manifold temperature 100°C, and detector temperature 100°C. The recorder was a Varian Model A-25 operated at one millivolt full scale and 0.25 in/min.

Gas sampling was accomplished with a Precision Sampling, Series A-2, 1.0-ml Pressure-Lok gas syringe, with 1.0-ml samples used throughout.

Calibration curves for oxygen, nitrogen and methane were generated by preparing a series of different, known pressures of these gases in 100-ml Pyrex® bulbs. Each bulb was equipped with a Kontes 4-mm Teflon® vacuum valve and a silicon rubber septum. Pressues were measured with a Texas Instruments Model 145 Precision Pressure Gauge, and helium was used to adjust the total pressure to 760 Torr. A typical gas chromatograph trace is shown in Figure 1. The actual calibration curves utilized are shown in Figure 2.

RESULTS

Four basic experiments were conducted in this phase of the research. In the first set of experiments, 1000 μℓ of MMH was added to the 300 ml bulb which contained 610 Torr of helium and 100 Torr of oxygen. MMH partial pressure at 25°C was found from the following equation (Reference 4).

$$\log_{10} P\ (\text{Torr}) = 7.11158 - \frac{1104.571}{(T,\ ^\circ K)} - \frac{152227.6}{(T,\ ^\circ K)^2}$$

to be 49.06 Torr.

The results of two experiments run with these conditions are shown in Figure 3. It can be estimated from this figure that for approximately every one mole of oxygen consumed in the reaction, 1.3 moles of nitrogen and one mole of methane were produced. The plots, however, do not conform to pseudo first order behavior, indicating that processes other than simple, homogeneous gas phase oxidation of MMH are occurring under these experimental conditions.

The second set of experiments in the 300-ml bulb was conducted with 31.6 μℓ MMH (34.4 Torr) injected into the bulb which contained 595 Torr of helium and 150 Torr of oxygen. This amount of MMH was well below the 49 Torr saturation point at 25°C, so all MMH was vaporized. These proportions gave about a four-fold oxygen concentration excess.

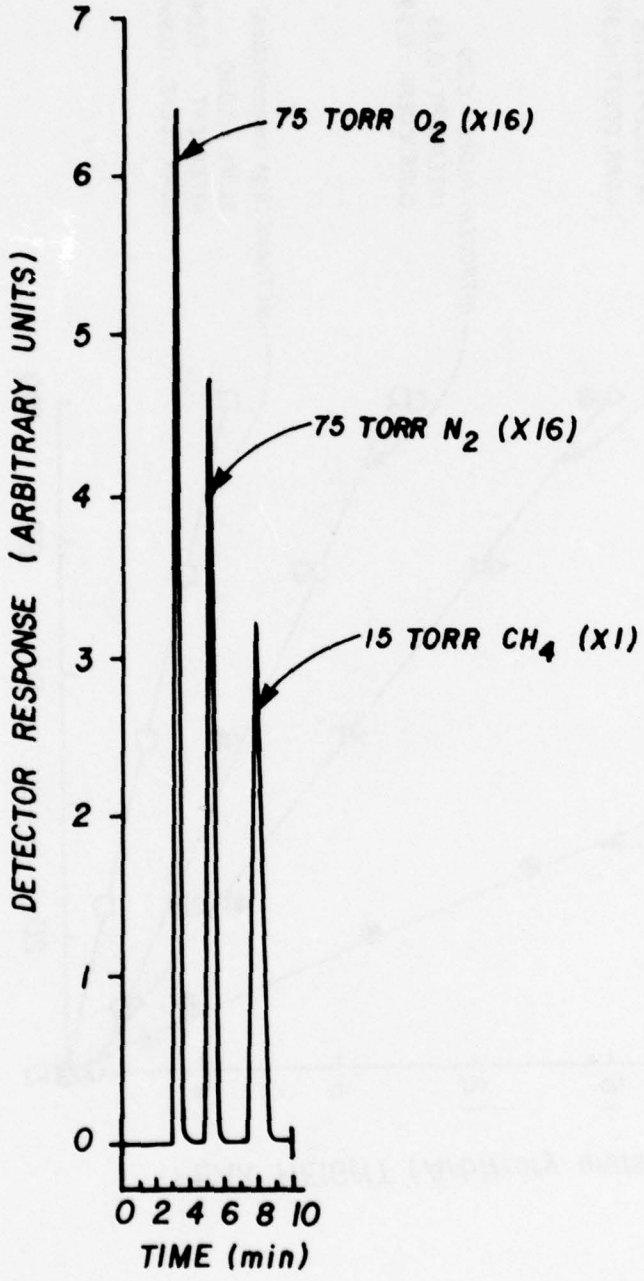

Figure 1. Chromatogram Showing Retention Times and Relative Response for Oxygen, Nitrogen and Methane

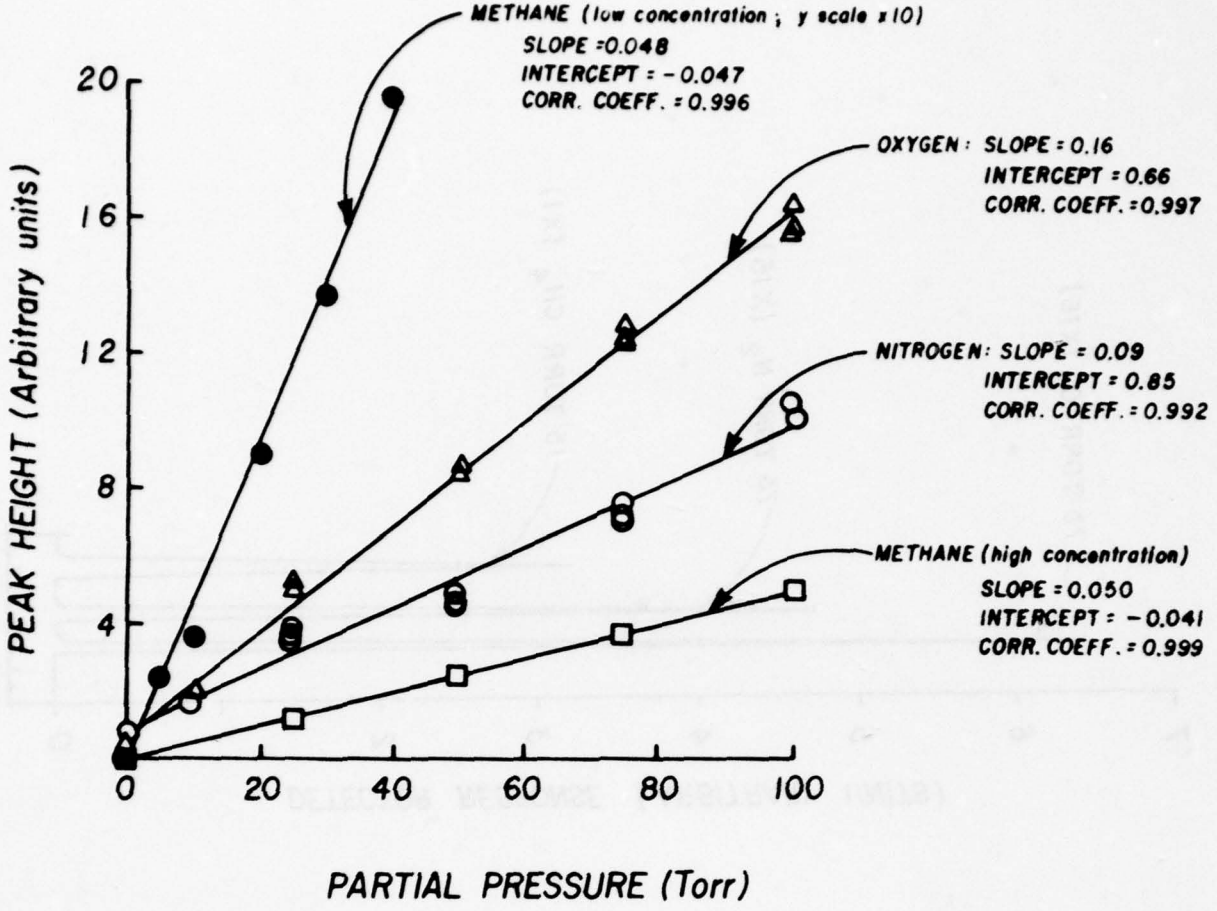

Figure 2. Calibration Curves for Oxygen, Nitrogen and Methane

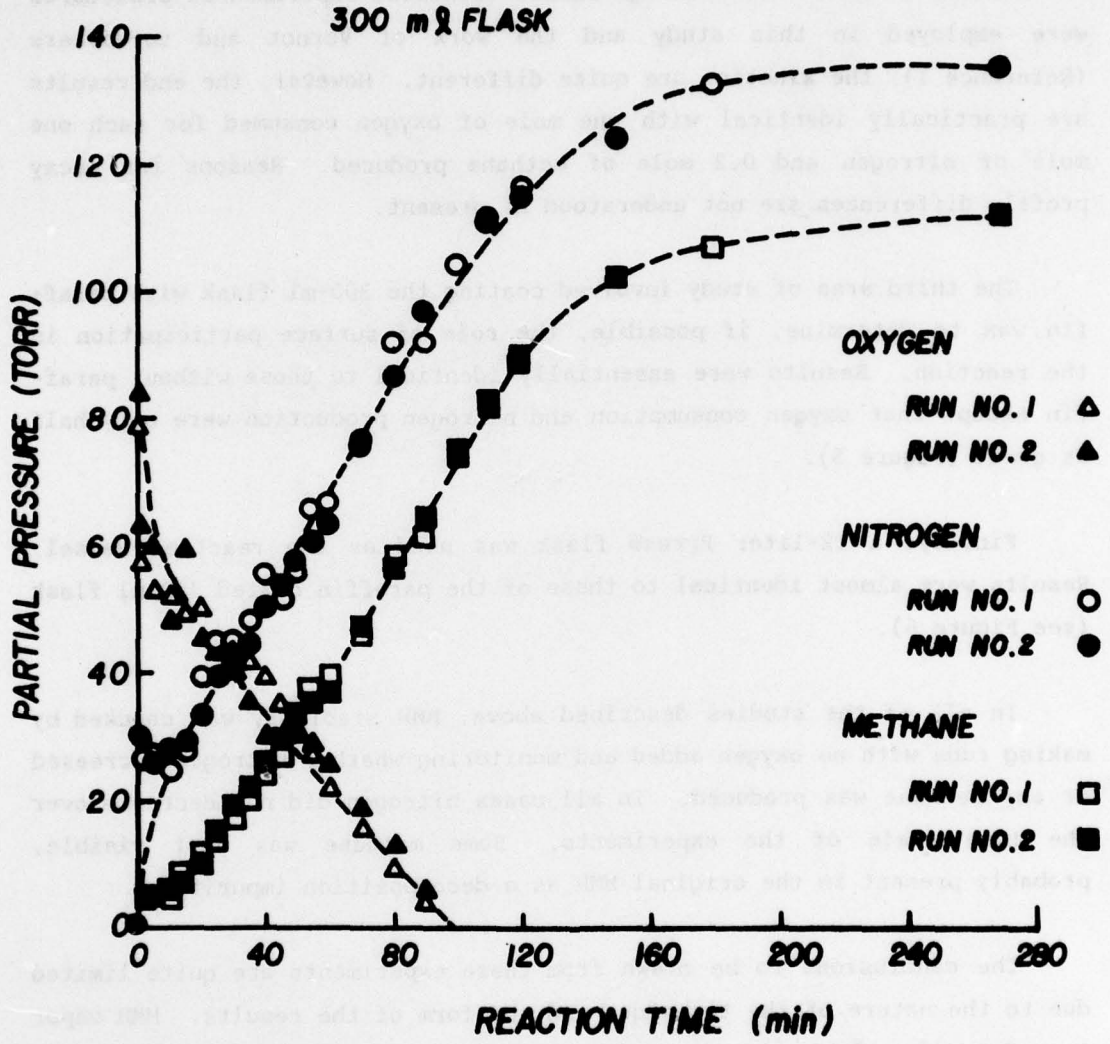

Figure 3. Plots of Oxygen Decay and Nitrogen and Methane Production versue Time in the 300-ml Bulb (Initial Conditions: 1000 µl MMH, 610 Torr Helium, and 100 Torr Oxygen)

Results are shown in Figure 4. It is not clear why the reaction seemed to go to essential completion within the first minute or so after MMH addition, however, this was consistently the case. Thus, reaction kinetic parameters were not able to be ascertained from these runs. It is of interest to note that although almost identical experimental procedures were employed in this study and the work of Vernot and co-workers (Reference 1), the kinetics are quite different. However, the end results are practically identical with one mole of oxygen consumed for each one mole of nitrogen and 0.2 mole of methane produced. Reasons for decay profile differences are not understood at present.

The third area of study involved coating the 300-ml flask with paraffin wax to determine, if possible, the role of surface participation in the reaction. Results were essentially identical to those without paraffin except that oxygen consumption and nitrogen production were only half as great (Figure 5).

Finally, a 12-liter Pyrex® flask was used as the reaction vessel. Results were almost identical to those of the paraffin coated 300-ml flask (see Figure 6).

In all of the studies described above, MMH stability was checked by making runs with no oxygen added and monitoring whether nitrogen decreased or any methane was produced. In all cases nitrogen did not decrease over the time scale of the experiments. Some methane was just visible, probably present in the original MMH as a decomposition impurity.

The conclusions to be drawn from these experiments are quite limited due to the nature of the technique and the form of the results. MMH vapor is relatively stable in the absence of oxygen. When oxygen is present, methane production is apparently a direct function of the MMH: O_2 ratio. Most of the reaction in the systems with an MMH:O_2 ratio of 1:4 occurs in the first one or two minutes. This fact, coupled with the observation that only 10 to 20 Torr of O_2 were consumed with 34.4 Torr of MMH available, suggests that one molecule of oxygen can cause destruction of more

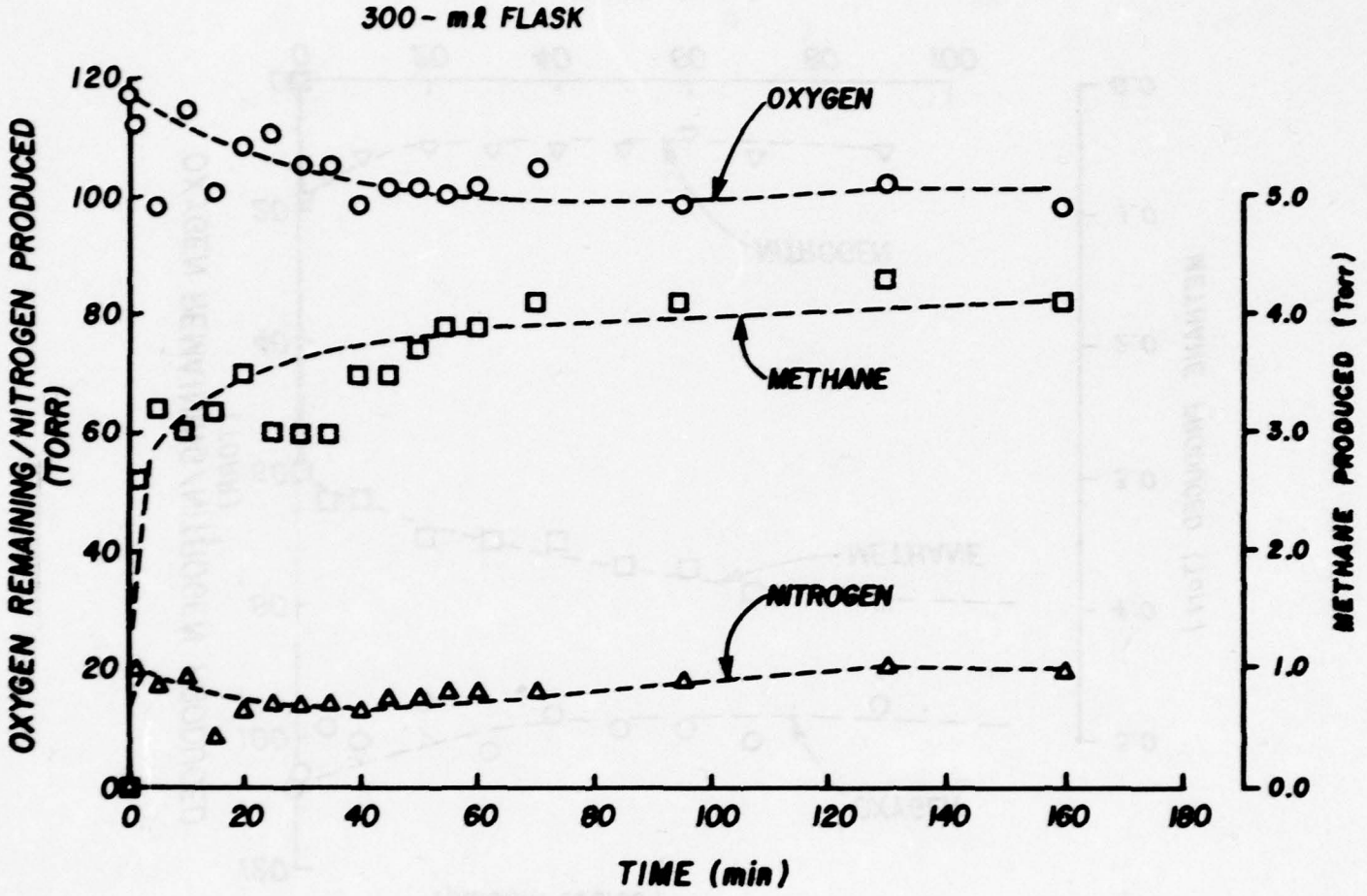

Figure 4. Plot of Oxygen Remaining and Nitrogen and Methane Production versus Time in the 300-ml (uncoated) Bulb (Initial Conditions: 31.6 µl MMH, 580 Torr Helium, 150 Torr Oxygen)

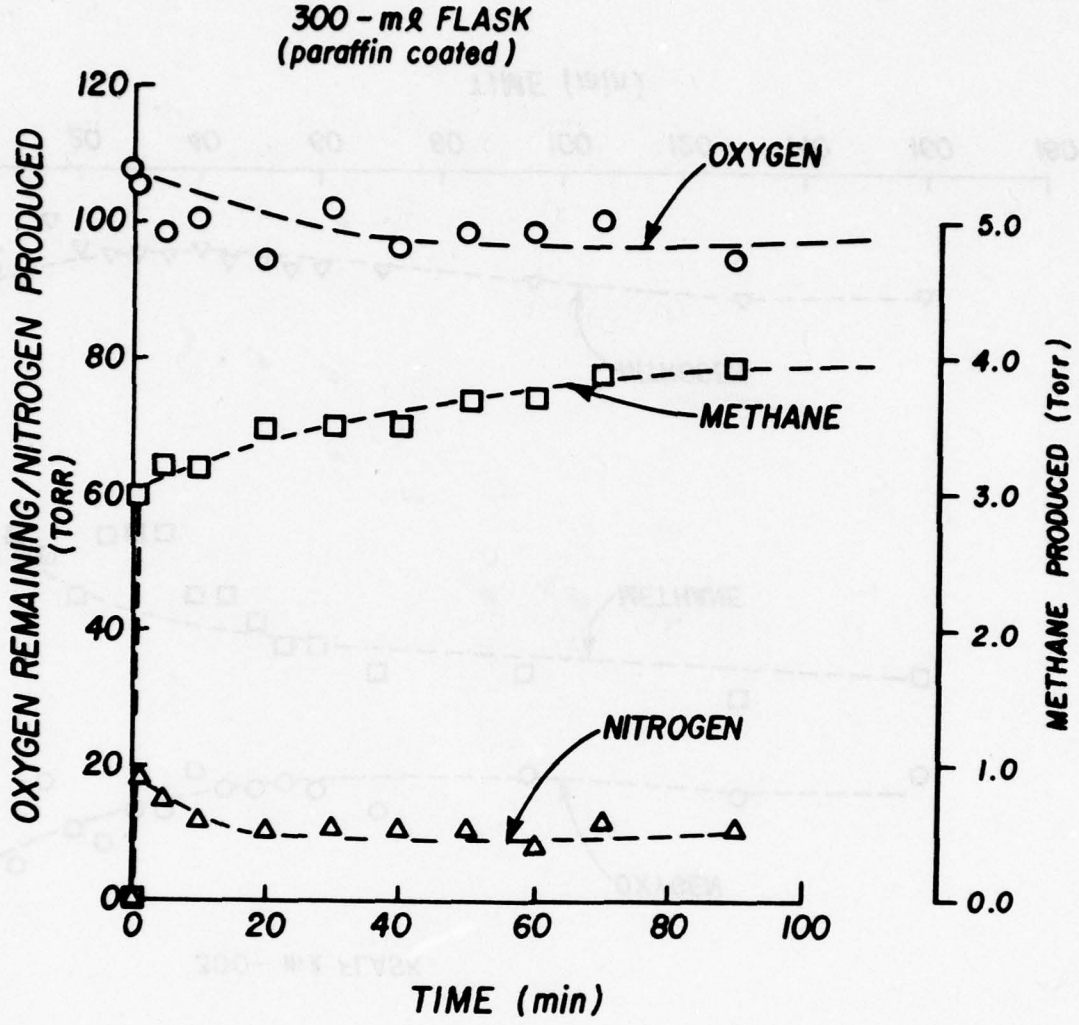

Figure 5. Plot of Oxygen Remaining and Nitrogen and Methane Production versus Time in the 300-ml (Paraffin Coated) Bulb, (Initial Conditions: 31.6 µl MMH, 580 Torr Helium, 150 Torr Oxygen).

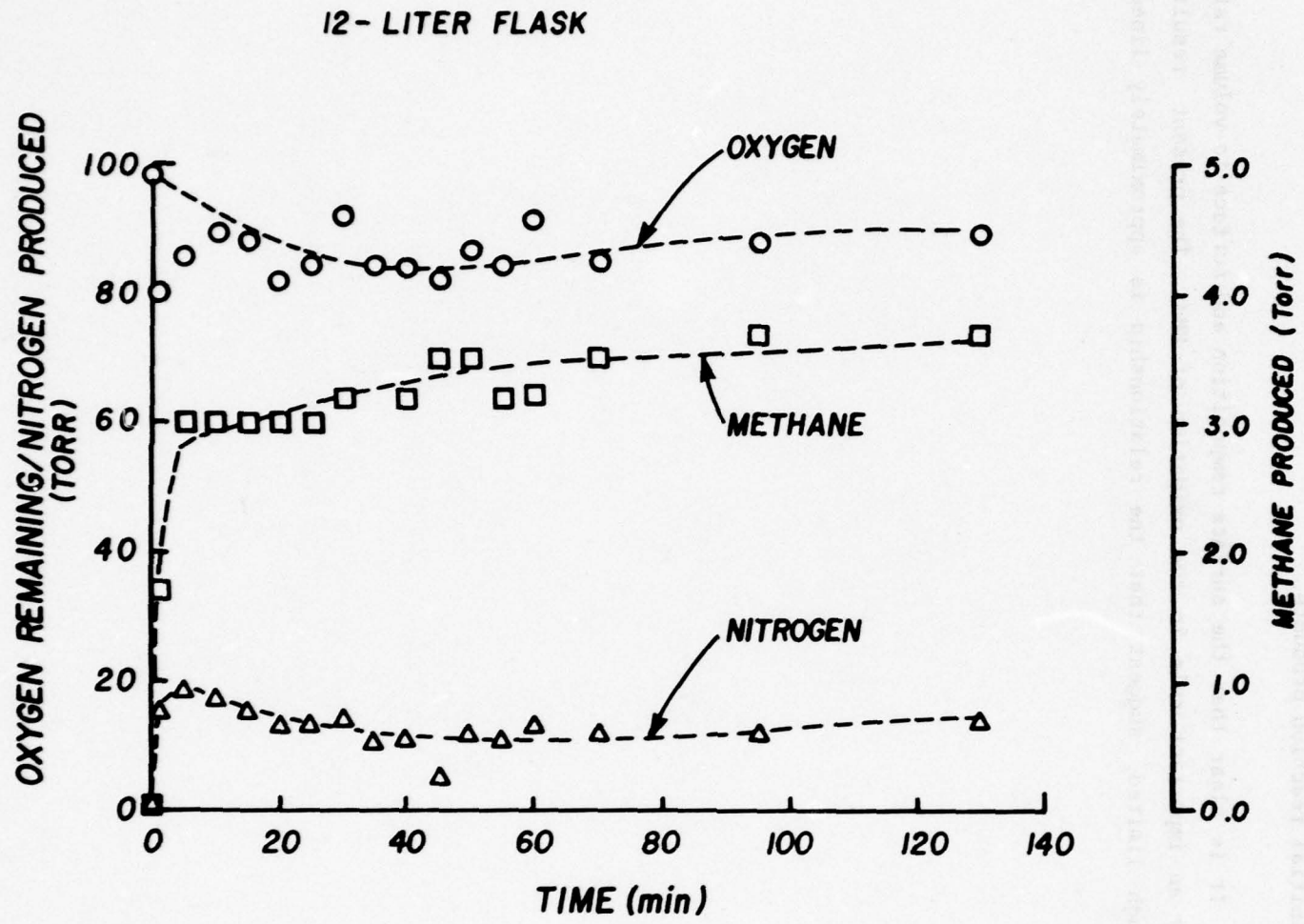

Figure 6. Plot of Oxygen Remaining and Nitrogen and Methane Production versus Time in the 12-Liter Flask (Initial Conditions: 1.16 ml MMH, 580 Torr Helium, 150 Torr Oxygen).

than one molecule of MMH, perhaps by some chain process. It is also possible that the oxygen was used up to some degree in further oxidation of initial reaction products.

It is clear that the surface composition and surface to volume ratio play an important role in the oxidation of MMH. The present results, though limited, suggest that the relationship is approximately linear.

SECTION IV

OXIDATION IN 44-CM PATH REACTION CELLS

EXPERIMENTAL

Three reaction cells of differing surface to volume (S/V) ratios but equal path lengths (44 cm) were used in this phase of the study. The infrared window mounting system is described in Reference 3. Flask volumes and S/V ratios were:

Volume (ℓ)	Surface to Volume Ratios (cm^{-1})
0.14	2.0
5.1	0.30
12	0.21

The infrared optical system used in this study has been described previously (Reference 3). Spectra were obtained at 4 cm^{-1} resolution with a Digilab Model FTS-20 Fourier transform infrared spectrophotometer. A Globar® source with a potassium bromide beamsplitter and a mercury-cadmium-telluride detector (operated at 77°K) were employed throughout this phase of the work.

All the experiments described in this section were conducted in the same manner. The cell was evacuated with a mechanical vacuum pump (Sargent-Welch Model 1402) while situated in position for infrared spectra to be recorded. Then about five Torr of MMH were expanded into the cell and the pressure was raised to 605 Torr with nitrogen (pressures were measured with Wallace and Tiernan Model FA16150, 0.1-20 Torr and Model FA160230, 0-800 Torr absolute pressure gauges respectively). The mixture was then allowed to equilibrate for 30 minutes. Spectra for beginning concentration determination were recorded at 30 and 45 minutes. Oxygen was then added to bring the total pressure to 760 Torr. At this point the

infrared spectrophotometer was set up to operate via paper tape execute commands and record absorbance spectra every 30 minutes, automatically, for six hours. These spectra were then plotted and used to derive the time history of the reaction.

MMH absorbance calibration spectra were recorded by expanding known pressures of MMH into the previously evacuated 5-liter flask, then bringing the total pressure to 760 Torr with nitrogen. Pressures were measured with a Texas Instruments Model 145 precision pressure gauge. Immediately after filling, the flask was transferred to its place in the infrared optical system and a spectrum was recorded at 2, 7, and 12 minutes. The absorbance decreased over this time period, so these three spectra were extrapolated to "zero time" by a 2nd order fit using the three absorbance versus time values. The "zero time" absorbance values were then used to derive the absorbance versus concentration curve shown in Figure 7. The analytical band used for concentration measurements was the A-type, NH_2 rocking fundamental at 888 cm^{-1} (Reference 5). A 4-cm^{-1} resolution spectrum of MMH is shown in Figure 8 with this band identified.

RESULTS

Several sets of experiments were conducted to determine MMH autoxidation kinetics in each reaction vessel. In Figure 9 the MMH decay in the 12-liter flask is plotted. It is evident that in the absence of oxygen MMH was stable on the time scale of the later oxidation run. With a "normal" atmosphere of 20 percent oxygen, the MMH decay was relatively slow with an estimated half-life of 400 to 450 minutes.

In Figure 10 the results of MMH autoxidation in the 5-liter flask are shown. Once again, the MMH is stable in this flask in the absence of oxygen. The addition of a 20 percent oxygen - 80 percent nitrogen mixture to MMH results in decay which has a rate dependent on the method used to clean the reaction vessel. When cleaning was accomplished by running the flask through a cycle of the glass annealing oven (heated to 1085°F), the

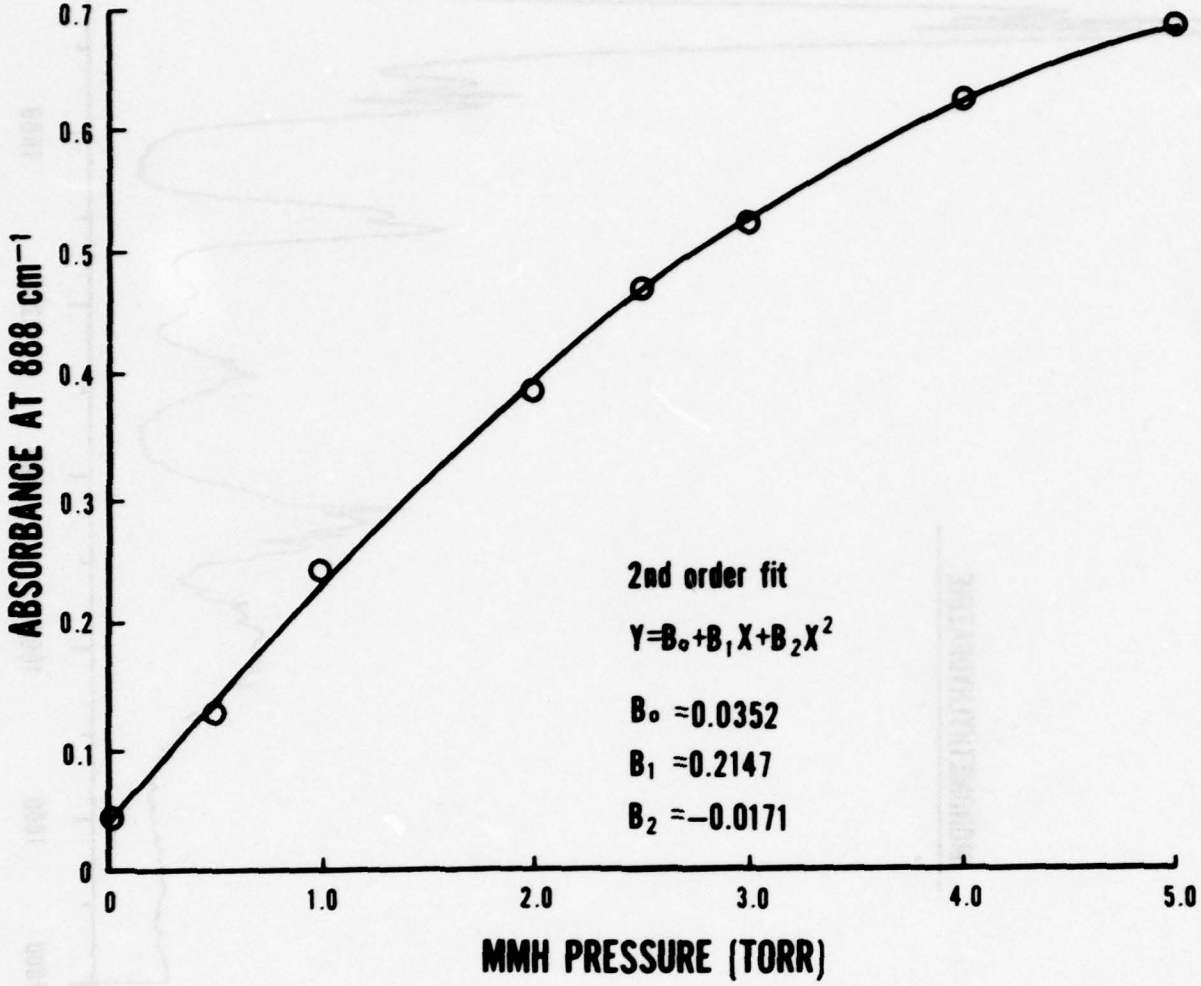

Figure 7. MMH Absorbance Calibration Curve (5-Liter Flask)

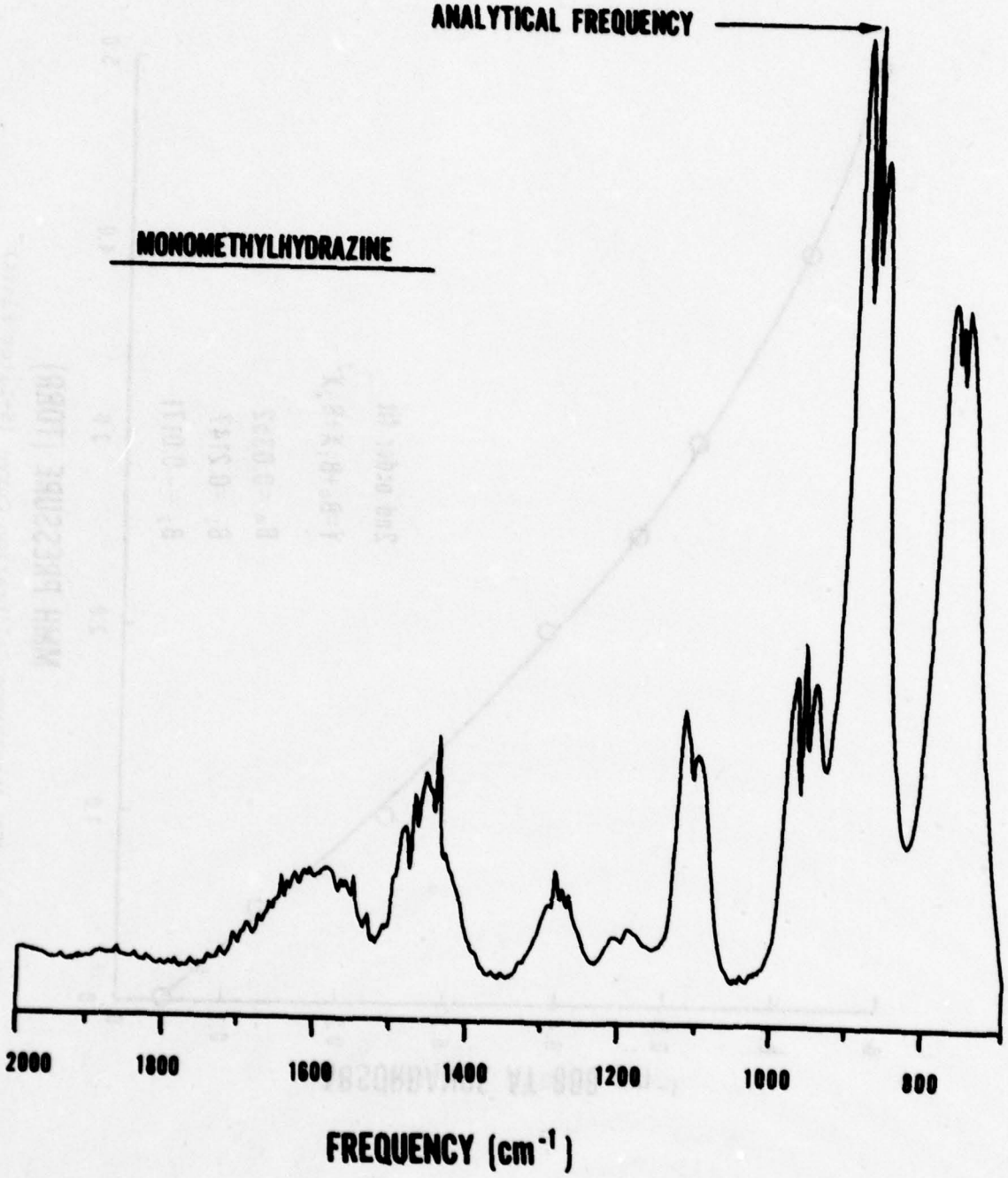

Figure 8. MMH Infrared Spectrum (4-cm^{-1} Resolution)

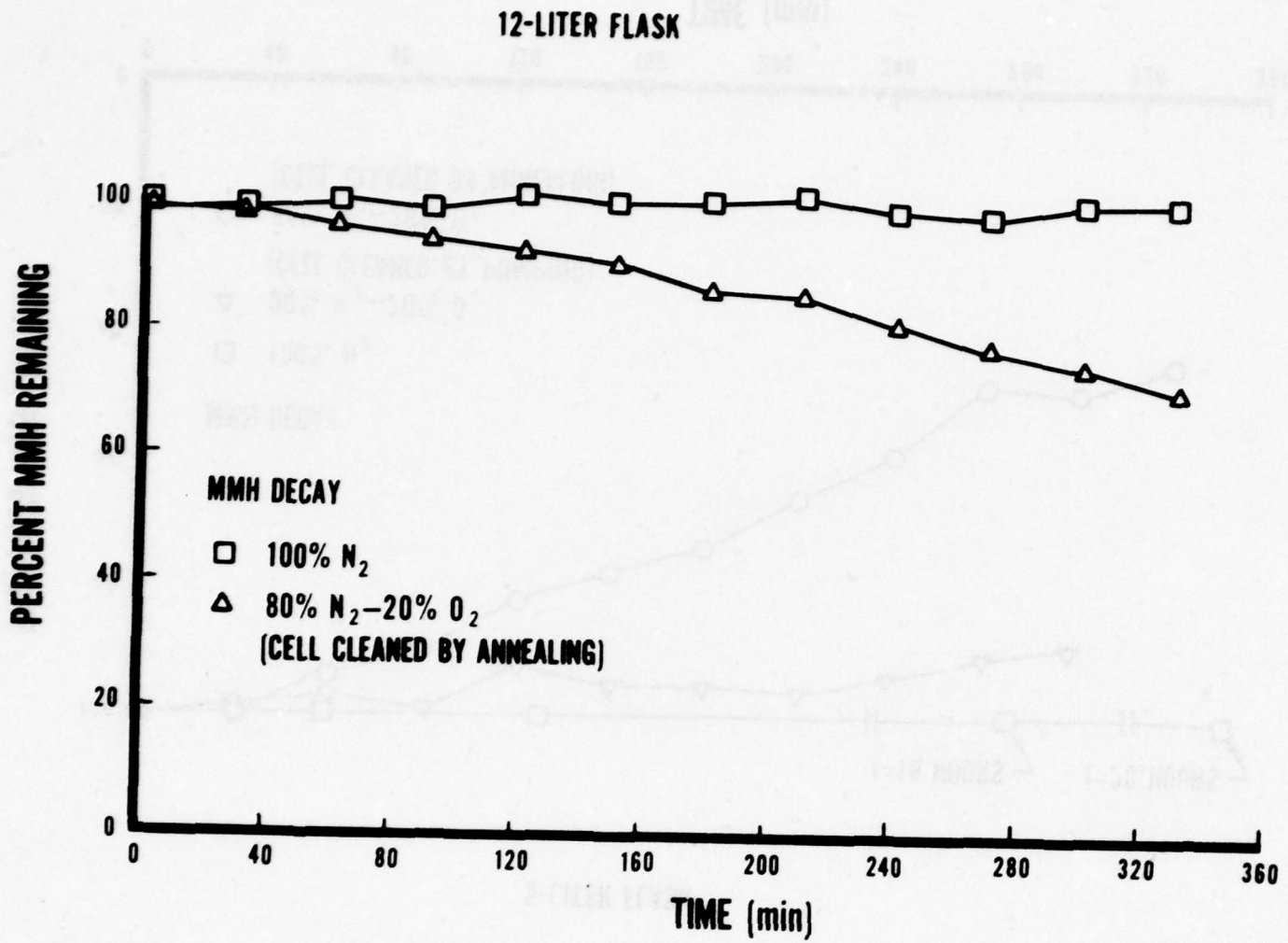

Figure 9. Plots of MMH Concentration versus Time for the 12-Liter Flask

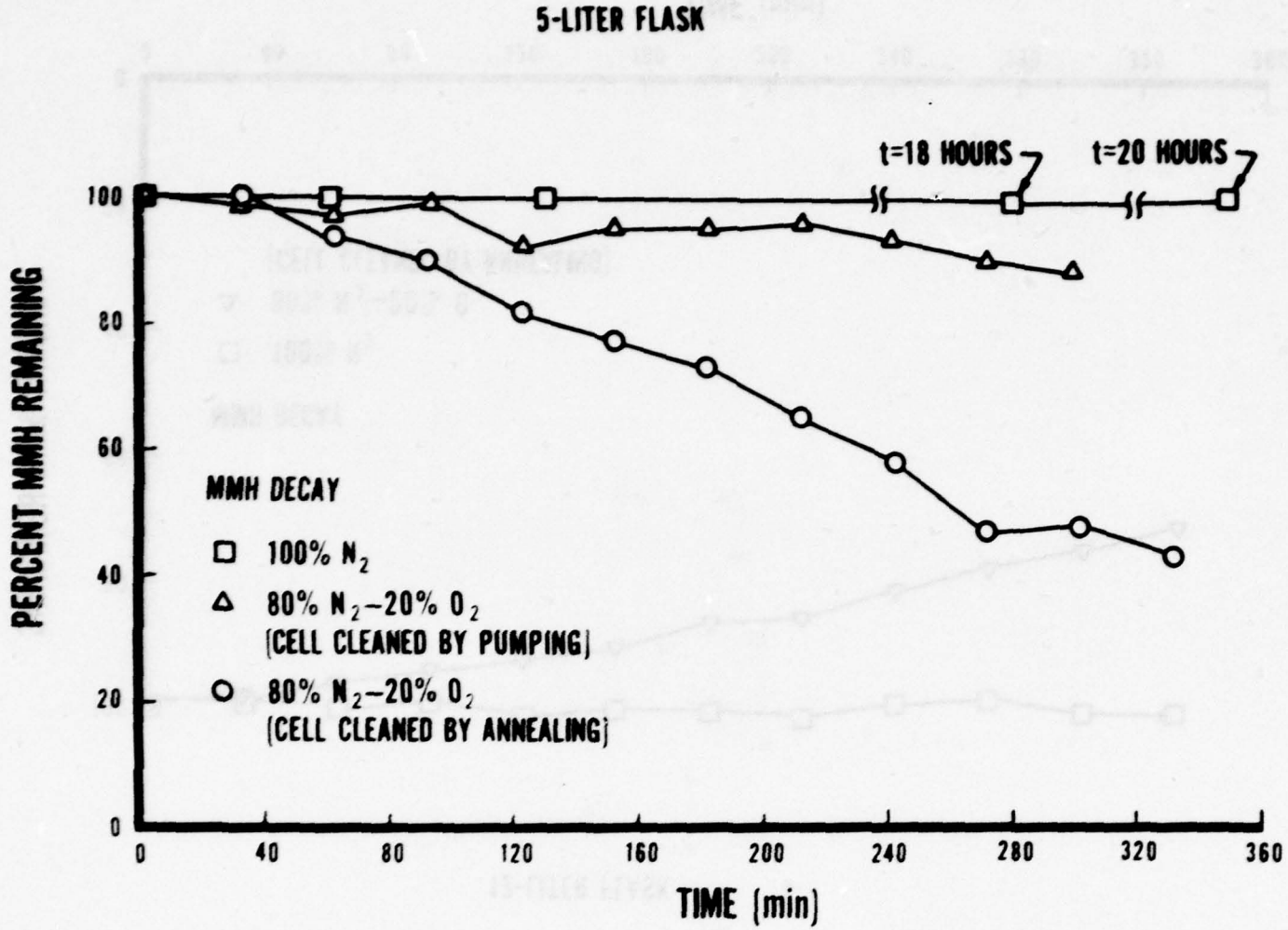

Figure 10. Plots of MMH Concentration versus Time for the 5-Liter Flask

oxidation proceeded much more rapidly than when cleaning was accomplished by pumping on the cell overnight. Clearly, heterogeneous processes are very important in this reaction vessel. The half-life in the annealed flask was around 260 minutes. In the flask cleaned by pumping, the half-life can only be estimated to be two to three times as long.

In the 44 x 2 cm cell, two sets of runs were made. In the first, the cell was used in the same experiments as the runs in the 5-liter flask. The results are plotted in Figure 11. In the absence of oxygen there was significant (~ 30%) loss of starting material over the course of the experiment. With the addition of synthetic air to MMH, the cell cleaned by pumping showed decay similar to that of the 5-liter cell, with a somewhat longer half-life of about 320 minutes. With cleaning accomplished by annealing, the decay profile changed to show an induction period of about an hour followed by a distinctly different, though more rapid decay profile than the cell cleaned by pumping.

In the second set of oxidation experiments (see Figure 12) in the 44 x 2 cm cell, 200 cm of 1/8-inch Teflon® tubing were added to the cell to approximately double the surface to volume ratio. In the cell cleaned by pumping, the decay rate was approximately doubled, with a half-life of about 160 minutes. In the cell cleaned by annealing (teflon tubing added after cleaning), the induction period was reduced, the reaction proceeded somewhat faster, but showed the same general decay profile as the run without the Teflon® tubing present.

These experiments demonstrate that the MMH oxidation rate is mostly controlled by heterogeneous processes with not only surface area, but also surface reactivity playing major roles in determining this rate. Oxidation of MMH could thus be expected to proceed in a similar manner in an enclosed area where similar concentrations of MMH were encountered.

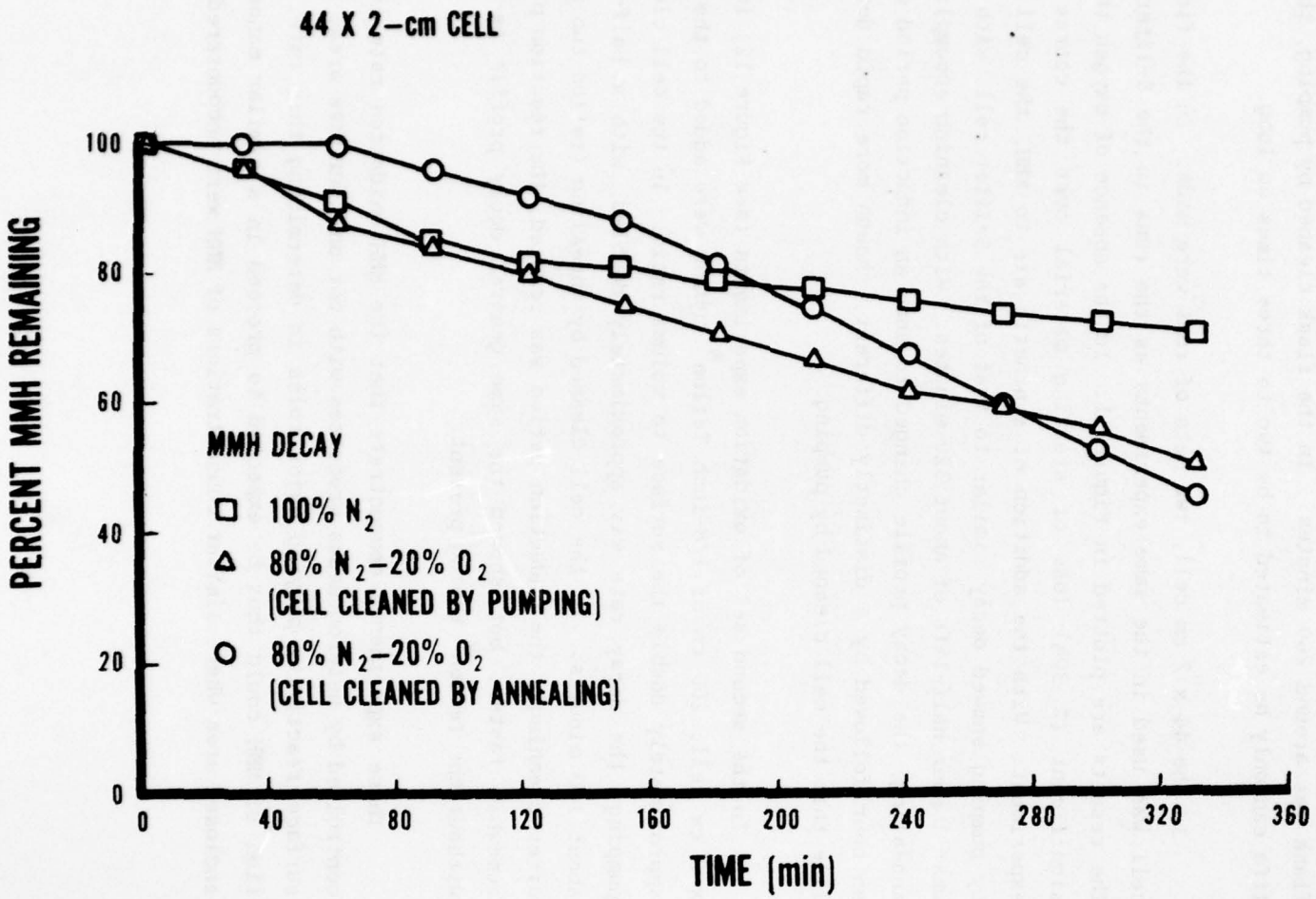

Figure 11. Plots of MMH Concentration versus Time for the 44 x 2-cm Cell

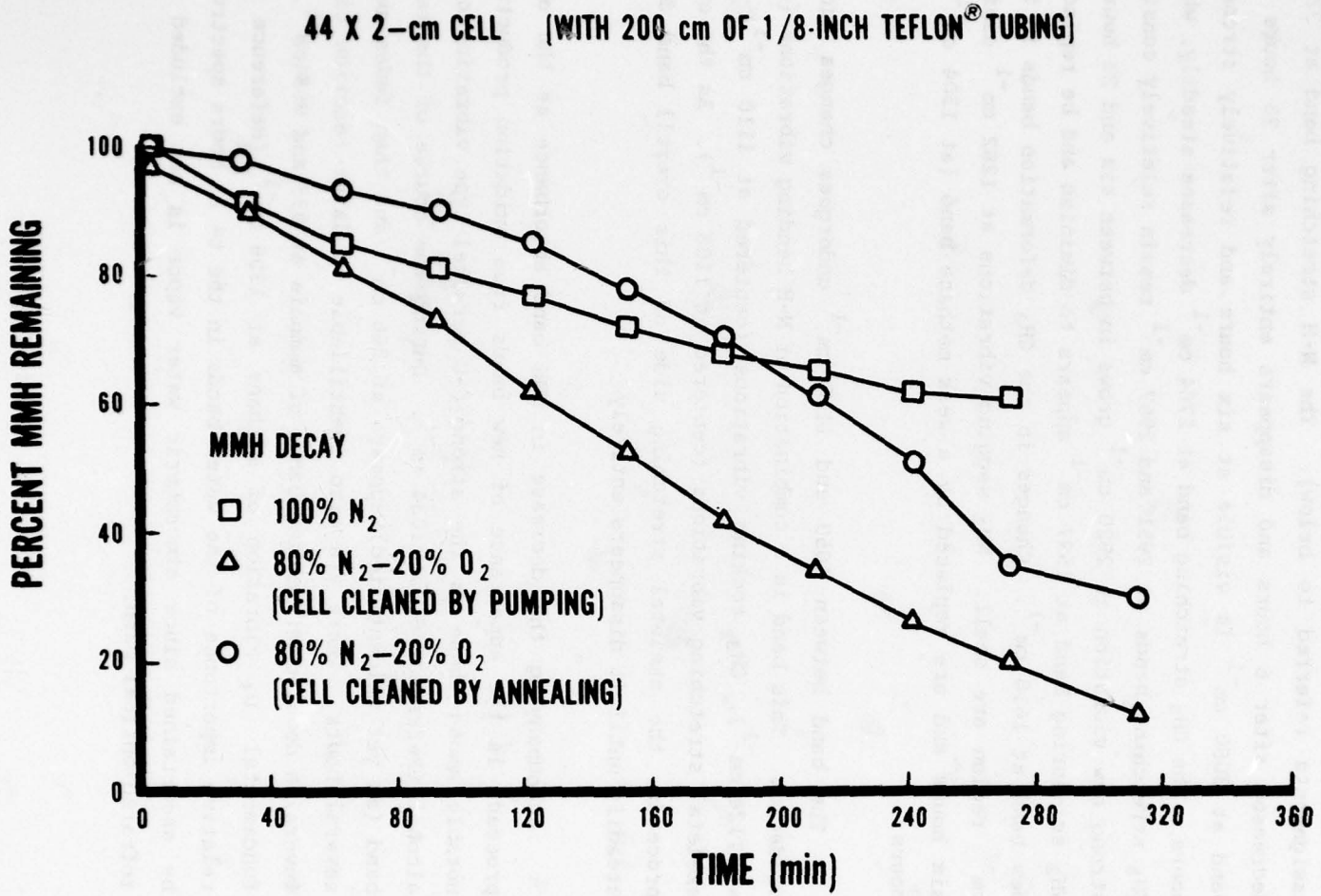

Figure 12. Plots of MMH Concentration versus Time for the 44 x 2-cm Cell (with Teflon® Tubing Added)

In Figure 13 a sequence of infrared spectra from a run in the 12-liter flask are shown. A number of changes in spectral features are visible as the reaction proceeds. (See Reference 5 for infrared band assignments referred to below). The N-H stretching band at 3260 cm^{-1} decreased after 6 hours and disappears entirely after 23 hours. A new band at 3080 cm^{-1} is visible at six hours and relatively strong at 23 hours. The CH_3 stretching band at 2784 cm^{-1} decreases steadily, while the CH_3 stretching bands at 2951 and 2967 cm^{-1} remain relatively constant. A strong new vibration at 2920 cm^{-1} grows in between six and 23 hours. The NH_2 scissoring band at 1597 cm^{-1} appears to diminish and be replaced by a new band at 1618 cm^{-1}. Changes in the CH_3 deformation bands in the 1450 cm^{-1} region are small. NH_2 wagging vibrations at 1282 cm^{-1} diminish at six hours and are replaced by a weak methane band (at 1304 cm^{-1}) at 23 hours.

The band between 1050 and 1150 cm^{-1} undergoes changes during the oxidation. This band is a combination of N-H bending vibrations (centered at 1124 cm^{-1}), CH_3 rocking vibrations (centered at 1118 cm^{-1}) and MMH skeletal stretching vibrations (centered at 1108 cm^{-1}). As the oxidation proceeds, the skeletal stretching side of this overall band decreases steadily until it disappears entirely.

Accompanying the decrease in MMH band absorbance as the oxidation proceeds is the appearance of new bands from oxidation products. Most notable among these is the strong C-O parallel-type vibration of methyl alcohol (Reference 6) at 1034 cm^{-1}. During the course of the reaction a band (as yet unidentified) appears at 846 cm^{-1} and then fades away after several hours. There are also identifiable at later reaction times, the inversion doubled NH bending bands of ammonia at 933 and 968 cm^{-1}, and the fundamental υ_4 vibration of methane at 1306 cm^{-1} (Reference 6). The relative importance of the water bands in the t= 23 hours spectrum cannot be ascertained since atmospheric water vapor is not excluded from the infrared optical path.

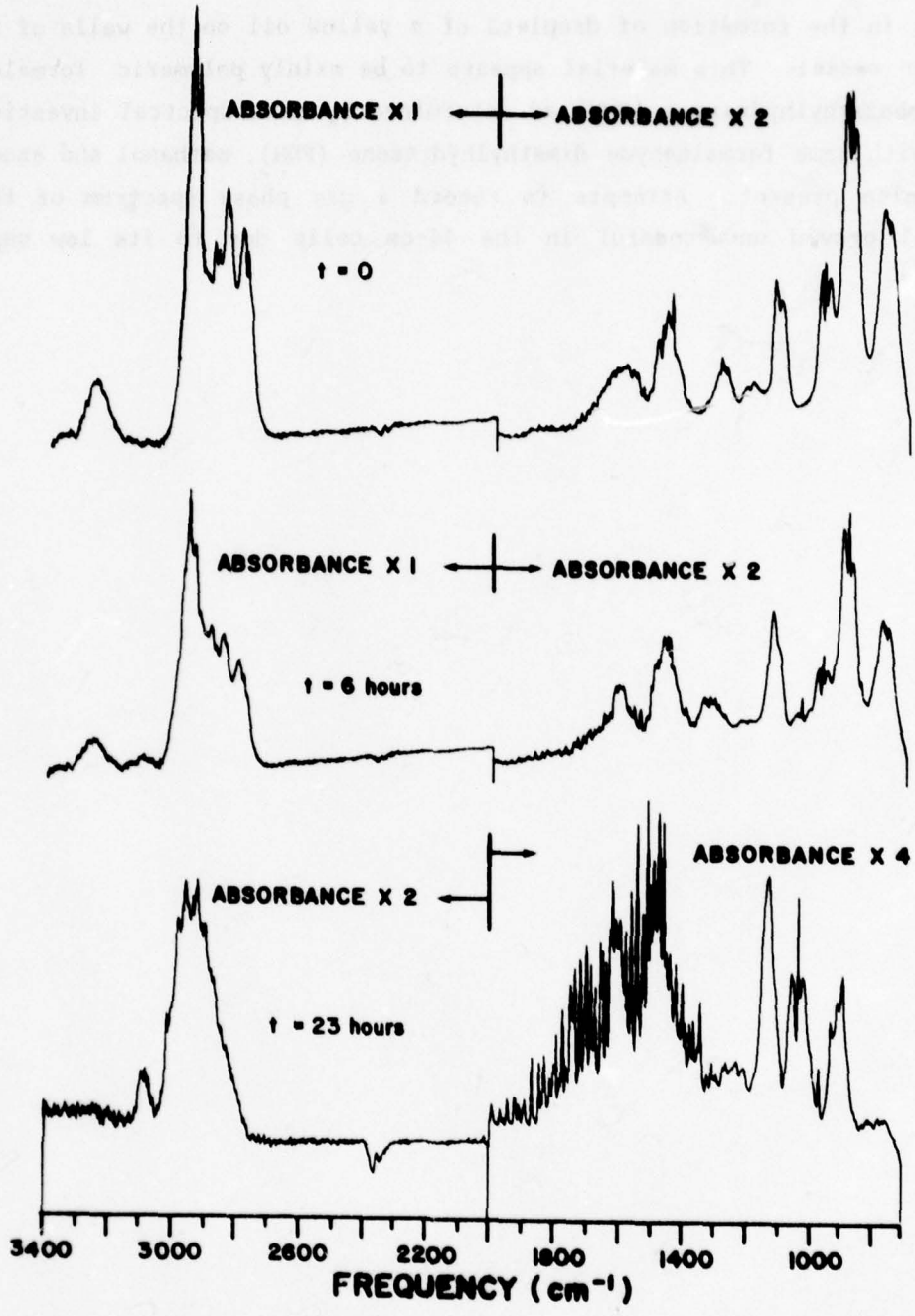

Figure 13. MMH Infrared Spectra Recorded During and Oxidation Run in the 12-Liter Flask (1.0-cm^{-1} Resolution)

In addition to these changes in infrared bands, the MMH oxidation results in the formation of droplets of a yellow oil on the walls of the reaction vessel. This material appears to be mainly polymeric formaldehyde monomethylhydrazone (FMH) as determined by mass spectral investigation, with some formaldehyde dimethylhydrazone (FDH), methanol and azomethane also present. Attempts to record a gas phase spectrum of this material proved unsuccessful in the 44-cm cells due to its low vapor pressure.

SECTION V

OXIDATION IN THE 55-LITER LONG PATH CELL

EXPERIMENTAL

The long path reaction cell employed in this phase of the experimental studies was constructed of a 0.152-meter by 3.05-meter section of Pyrex® pipe. Three mirror White-type (Reference 7) multiple-pass optics were installed in Plexiglass® mounts in the cell at a 2.75 meter separation. The cell was operated at 72 passes during this study for a path-length of about 200 meters. The White cell optics were coupled to a Digilab Model FTS-20 Fourier transform infrared spectrophotometer as shown in Figure 14. Spectra were recorded at 1.0 cm^{-1} resolution, using 64 coadded scans and triangular apodization.

Path length measurements were carried out by removing mirror M from the optical path (see Figure 14) and replacing it with a helium-neon laser. With the aid of this laser, mirrors II were adjusted to give two rows of images on mirror I corresponding to the desired number passes of the laser beam through the cell. The mirrors at II were adjusted to give 18 laser dots across one row of images on mirrow I. This corresponded to 4 x 18 or 72 passes through the cell for a total path length of 198 meters. With this adjustment complete, mirror M was replaced and adjusted to give maximum signal.

When set at long path lengths, the White cell type of optics are, naturally, very sensitive to small changes in the position of the mirrors marked II in Figure 14. In order to verify the path length without disturbing mirror M, methane was used as a path length measurement standard. The band at 1304 cm^{-1} was used with a Beer's law calculation where the molar extinction coefficient was that of Hanst, et. al. (Reference 8) 11 atm^{-1} cm^{-1}. The methane was obtained from a calibrated standard cylinder of 5.4 ppm methane in helium. The spectrum was recorded at

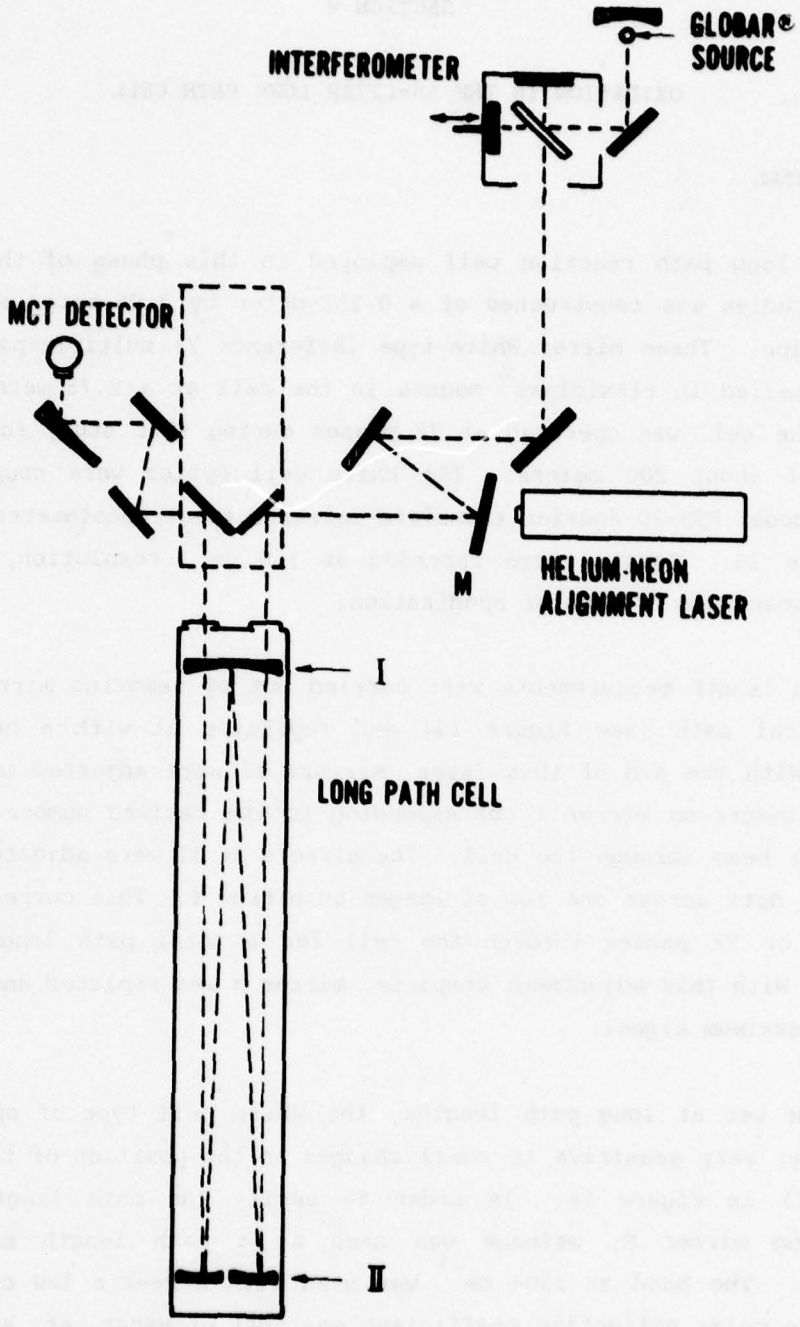

Figure 14. Optical Path Used in Conjunction with the Long Path Cell

760 Torr total pressure with 1.0 cm^{-1} resolution, thus giving the same conditions as those employed by Hanst and Co-workers. Agreement between the measured path length and that computed from counting laser dots was generally very good, with the measured values always somewhat less than the laser dot value.

Materials were introduced into the long path cell via an attached vacuum manifold, either through a silicon septum on the manifold with a syringe or by attaching a glass bulb with teflon valves at both ends to the manifold and flushing the contents into the cell with fill gas.

In order to determine the molar extinction coefficient for monomethylhydrazine in the 0-10 ppm range, the following procedure was employed. First MMH vapor was expanded from a glass storage bulb attached to a conventional high-vacuum system into a previously evacuated, double-ended transfer bulb of known volume. The pressure was measured with a Texas Instruments Model 145 precision pressure gauge. Then the pressure was raised to 760 Torr with helium. The bulb was then connected to the long path cell manifold and flushed into the cell with helium containing 5.4 ppm CH_4. A spectrum was then recorded at 1.0 cm^{-1} resolution by coadding 64 scans and ratioing them against the reference spectrum of the cell filled with pure helium. The resulting spectrum was plotted. Methane was used to determine the path length for each different sample of MMH. Then by plotting absorbance (at 888 cm^{-1}) versus the concentration (in ppm) times the path length (in cm) the slope of the resulting line multiplied by $\log_e$ (10) is the molar extinction coefficient. This plot is shown in Figure 15. This extinction coefficient was then used in subsequent MMH oxidation experiments to determine MMH concentration.

A typical MMH oxidation run was conducted as follows. The long path cell was adjusted to around 200 meters path length and the value was measured using a methane calibration standard. Then a measured amount of MMH was introduced into the evacuated long path cell in the manner described above, and helium was added to bring the total pressure to 610

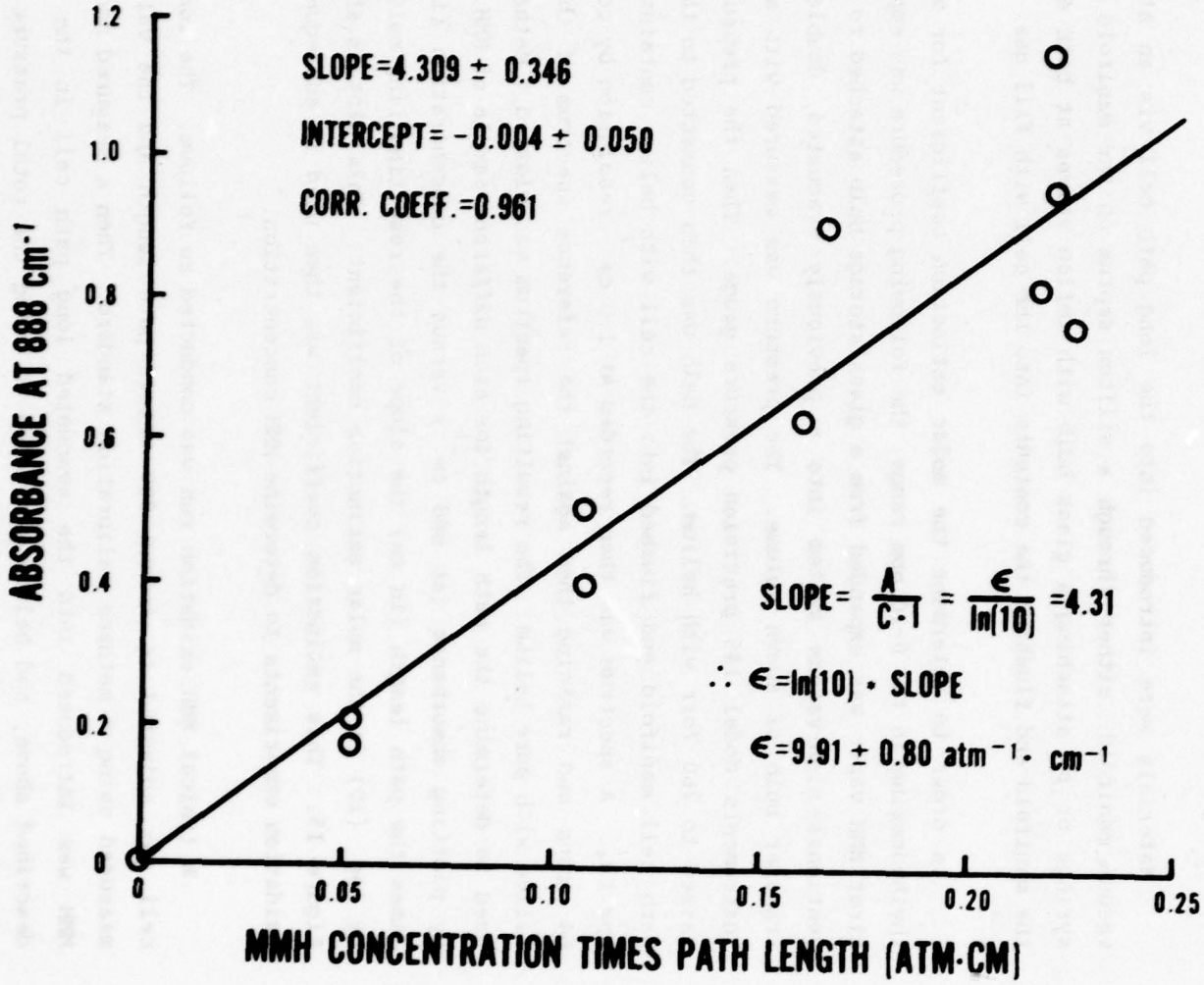

Figure 15. Plot of MMH Absorbance versus the Concentration - Path Length Product for Molar Extinction Coefficient Determination

Torr. The MMH was allowed to sit for 40 minutes to stabilize, then an initial MMH spectrum was recorded. Then oxygen was added to 760 Torr and the FT-IR spectrophotometer was set up to automatically acquire spectra every 60 minutes. The reaction was followed for five hours and then a final spectrum was recorded the next day after about 22 hours. These spectra were then plotted and MMH concentration versus time plots were made up.

RESULTS

Unlike the oxidation experiments conducted at Torr-level MMH partial pressures, those carried out in the long path cell at ppm-level MMH partial pressures displayed linear pseudo first order decay curves, as seen in Figure 16. Despite this difference, the stability and half-life of MMH in the long path cell were similar to runs in the 44-cm cells described earlier. This result seems to indicate that the same principal oxidation/decay mechanisms are operating in both systems.

Spectral changes described earlier for MMH oxidation reactions in the 44-cm cells were also observed in the long path cell. Production of methanol and methane were clearly visible. These two products account for around 30 percent of the original MMH carbon. The fate of the remaining 70 percent is quite uncertain. However, earlier studies at higher MMH concentration and a similar study on 1,1-dimethylhydrazine (Reference 9) suggest that most of the remaining 70 percent is probably formaldehyde monomethylhydrazone (FMH) along with some formaldehyde dimethylhydrazone (FDH), formaldehyde hydrazone (FH) and azomethane. The MMH nitrogen is probably accounted for mostly by molecular nitrogen formation with the remainder essentially FMH. Unfortunately, none of these materials appear to account for the observed gas phase spectrum of MMH + 0_2 after reacting overnight. This observation came as a result of comparing spectra of FMH (Figure 17), FDH (Figure 18), and FH (Figure 19) (synthesized by bubbling formaldehyde vapor through MMH, UDMH and hydrazine respectively) obtained at ppm partial pressures in the long path cell, and azomethane from

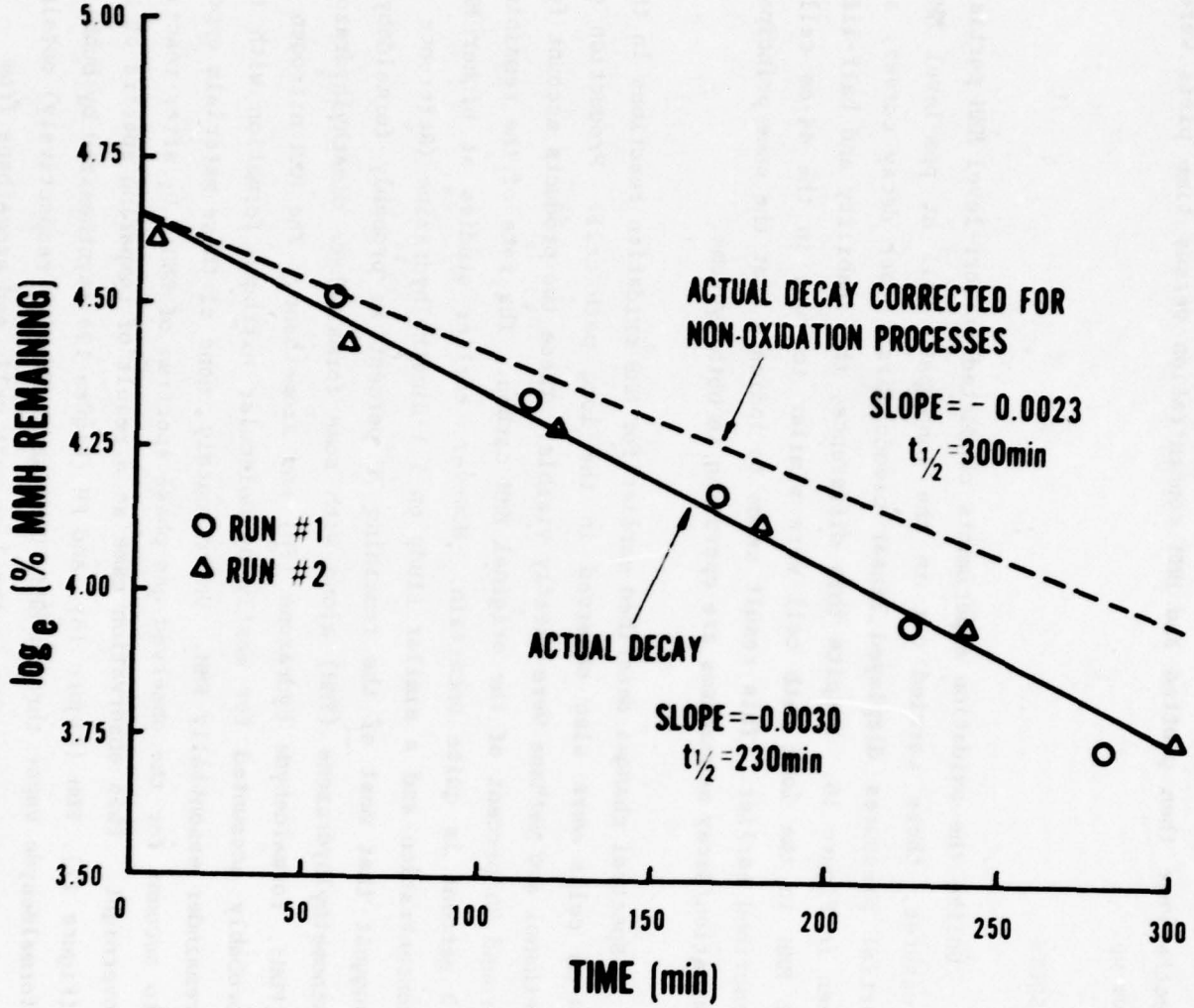

Figure 16. Plot of Log_e Percent MMH Remaining versus Time Showing Pseudo First Order Behavior as well as the Correction for Non-Oxidation Decay Processes

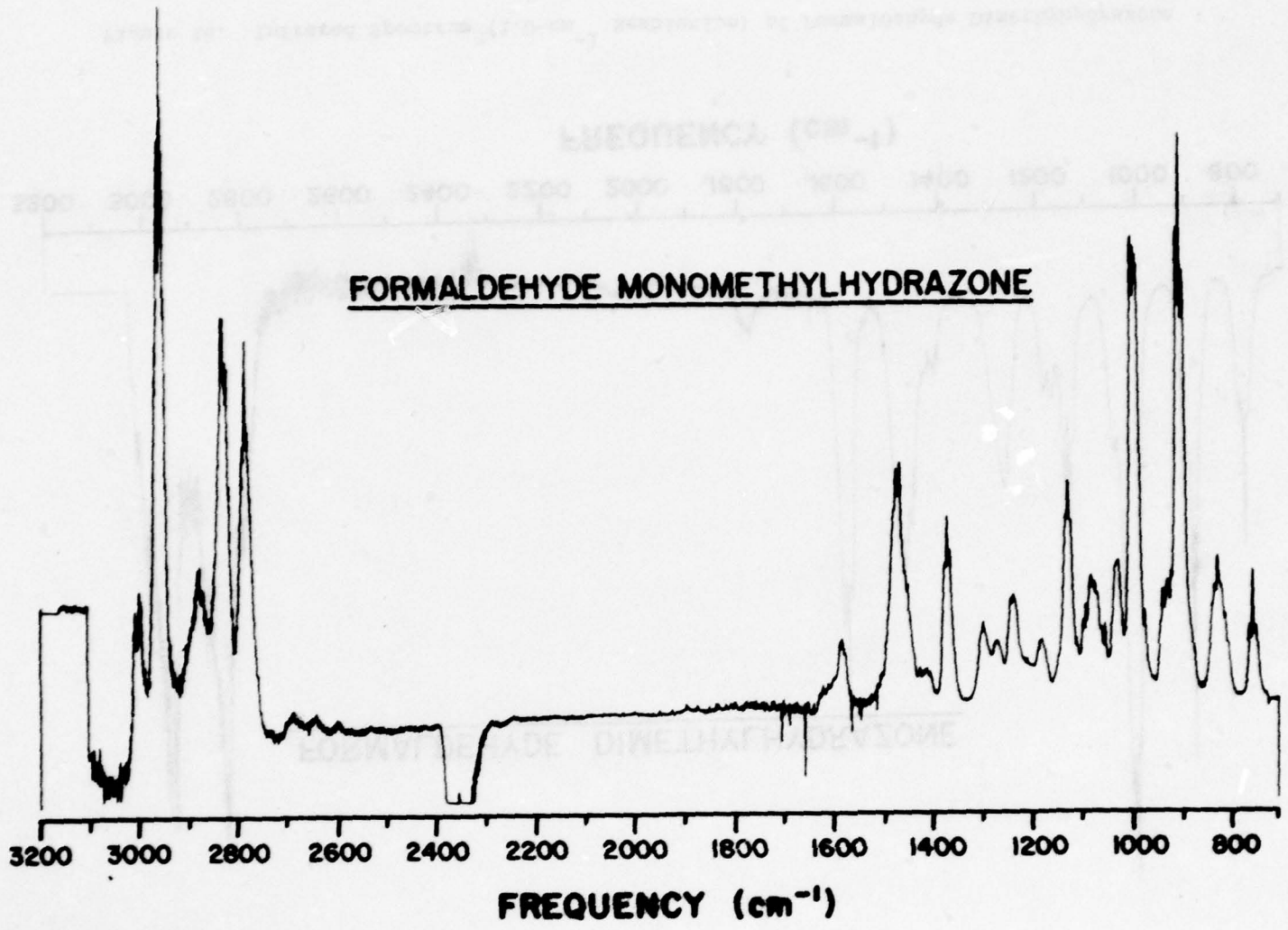

Figure 17. Infrared Spectrum (1.0-cm^{-1} Resolution) of Formaldehyde Monemethylhydrazone

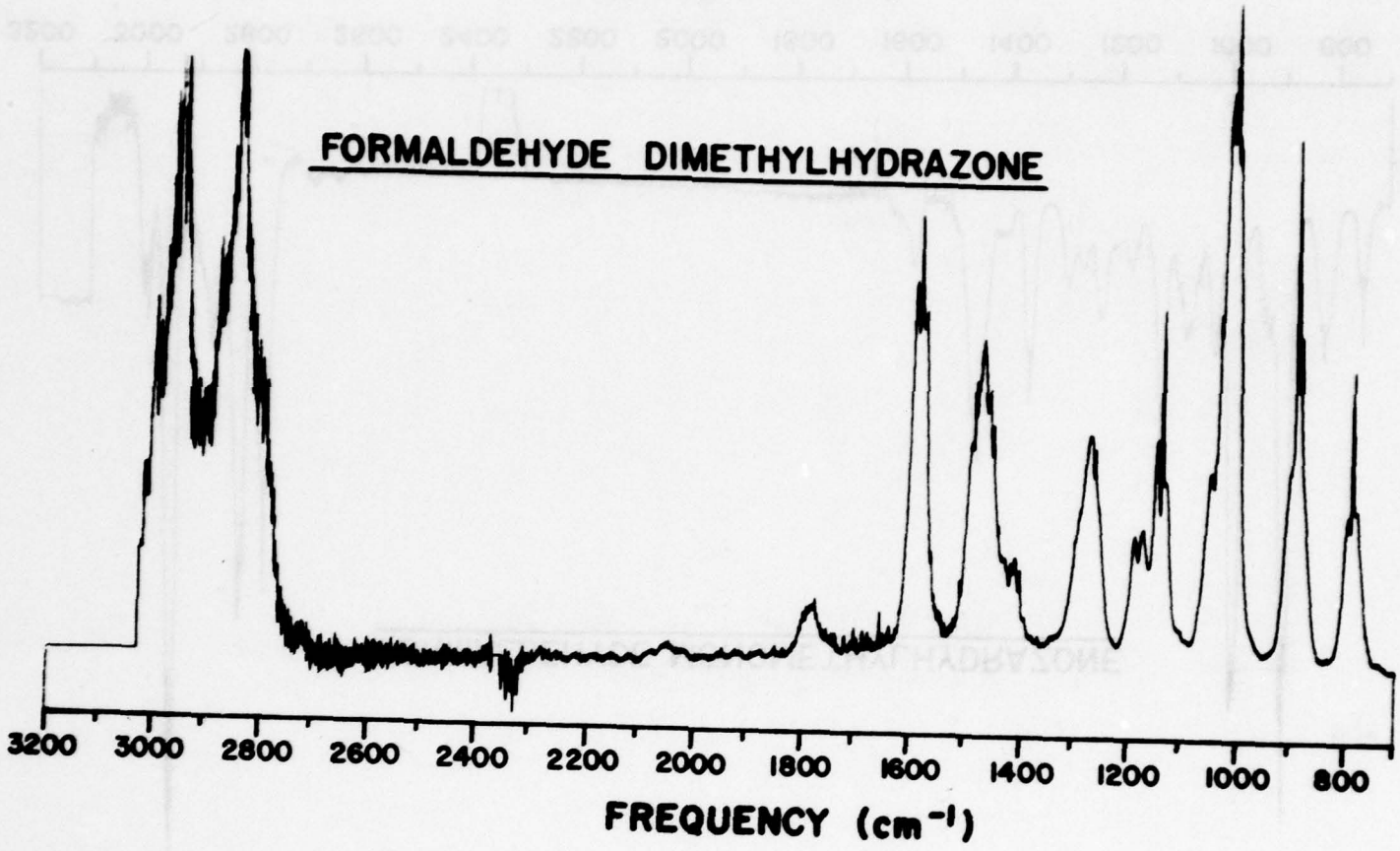

Figure 18. Infrared Spectrum (1.0-cm^{-1} Resolution) of Formaldehyde Dimethyhydrazone

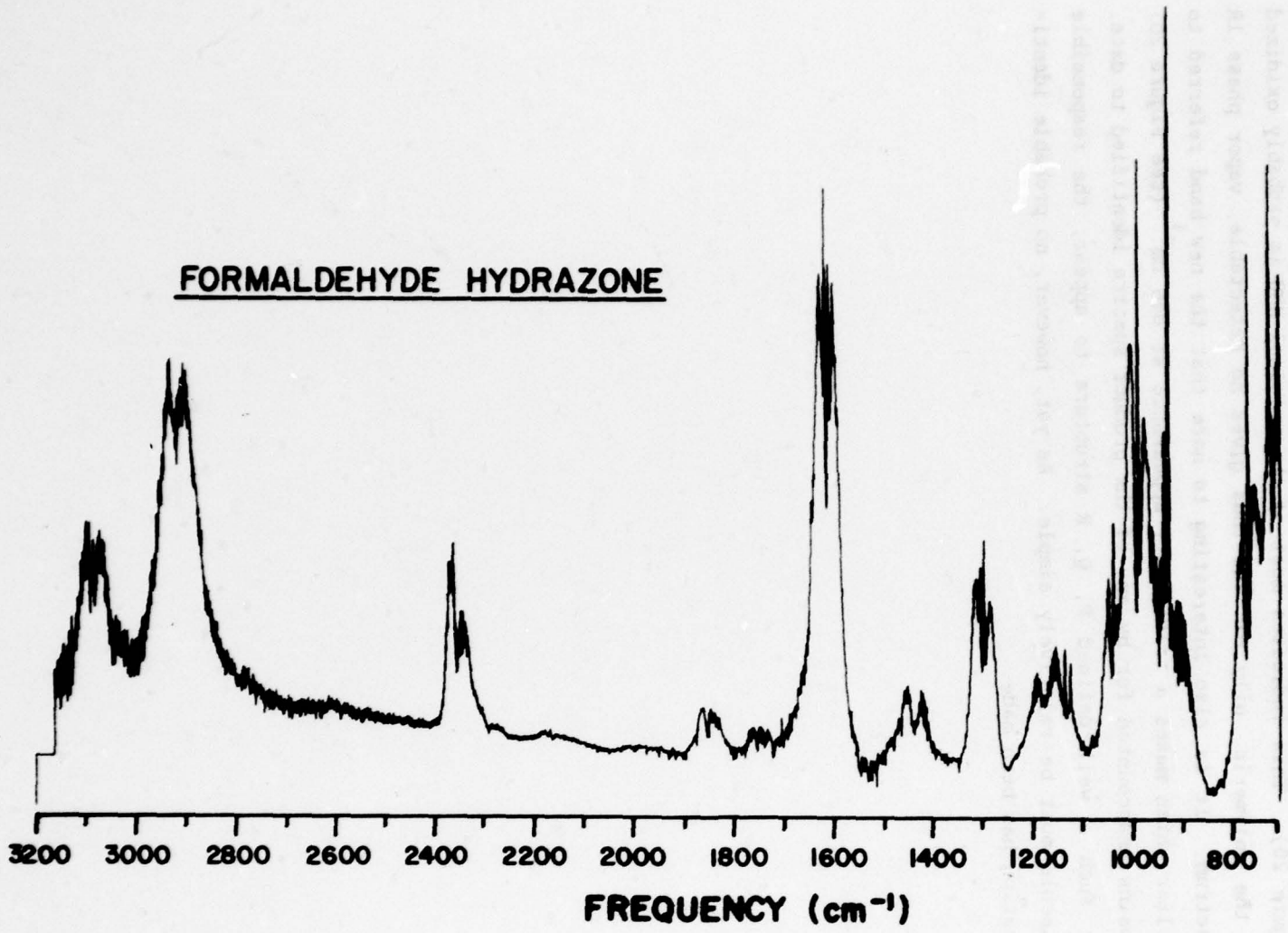

Figure 19. Infrared Spectrum (1.0-cm^{-1} Resolution) of Formaldehyde Hydrazone (Note: Atmospheric CO_2 is Also Present)

Reference 10, with the observed spectrum of the MMH + O_2 system (see Figure 20). This indicates most of the original MMH is probably oxidized to the polymeric, oily FMH and thus gives no detectable, vapor phase IR spectrum. It is also interesting to note that the new band referred to earlier which makes a transistory appearance at 846 cm^{-1} (see Figure 20) remains unaccounted for by any of the product spectra identified to date. For such a well defined P, Q, R structure to appear, the responsible molecule must be relatively simple. As yet, however, no probable identification has been made.

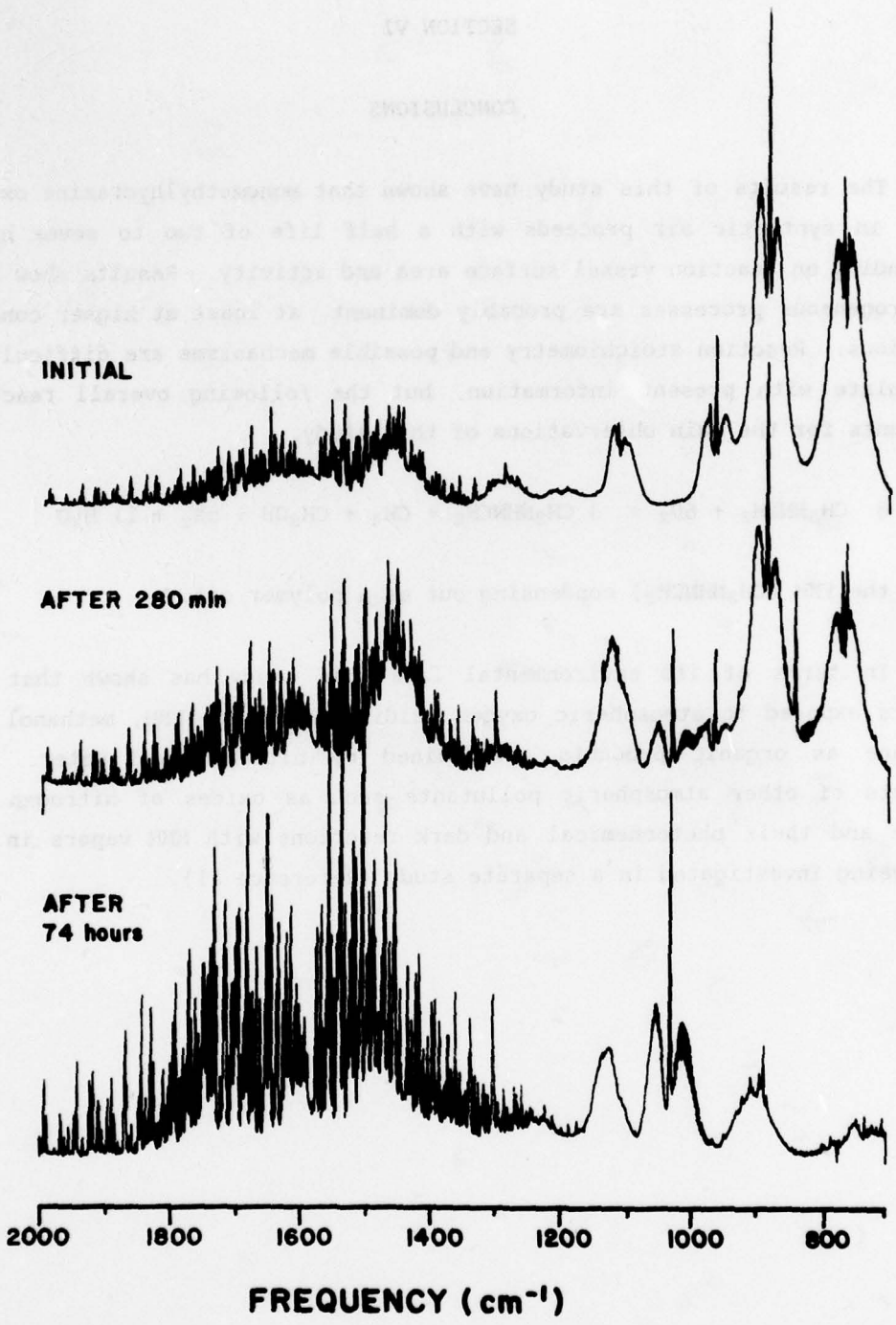

Figure 20. MMH Infrared Spectra Recorded During an Oxidation Run in the Long Path Cell (1.0-cm^{-1} Resolution)

SECTION VI

CONCLUSIONS

The results of this study have shown that monomethylhydrazine oxidation in synthetic air proceeds with a half life of two to seven hours depending on reaction vessel surface area and activity. Results show that heterogeneous processes are probably dominant, at least at higher concentrations. Reaction stoichiometry and possible mechanisms are difficult to postulate with present information, but the following overall reaction accounts for the main observations of this study.

$$8\ CH_3NHNH_2 + 6O_2 \rightarrow 3\ CH_3NHNCH_2 + CH_4 + CH_3OH + 5N_2 + 11\ H_2O$$

with the FMH (CH_3NHNCH_2) condensing out as a polymer oil.

In terms of its environmental fate this study has shown that MMH vapors exposed to atmospheric oxygen oxidize mainly to FMH, methanol and methane as organic products accompained by nitrogen and water. The effects of other atmospheric pollutants such as oxides of nitrogen and ozone and their photochemical and dark reactions with MMH vapors in air are being investigated in a separate study (Reference 11).

REFERENCES

1. Vernot, E. H., MacEwen, J.D., Geiger, D.L. and Haun, C. C., "The Air Oxidation of Monomethyl Hydrazine," American Industrial Hygiene Association Journal, 28, 343 (1967).

2. Saunders, R.A. and Larkins, J.T., "Detection and Monitoring of Hydrazine, Monomethylhydrazine, and Their Decomposition Products," Naval Research Laboratory Memorandum Report 3313, Washington, D.C., June 1976.

3. Stone, D.A., "Autoxidation of Hydrazine Vapor," CEEDO-TR-78-17, Jan 1978.

4. Marsh, W.B. and Knox, B.K., USAF Propellant Handbooks Hydrazine Fuels, Vol. 1, AFRPL-TR-69-149, Mar 1970.

5. Durig, J.R., Harris, W.C. and Wertz, D.W., "Infrared and Raman Spectra of Substituted Hydrazines I. Methylhydrazine," The Journal of Chemical Physics, 50, 1449 (1969).

6. Herzberg, G.H., Molecular Spectra and Molecular Structure III. Infrared and Raman Spectra of Polyatomic Molecules, Van Nostrand Reinhold Co., New York, 1945.

7. White, J.L., "Long Optical Paths at Large Operture," Journal of the Optical Society of America, 32, 285 (1942).

8. Hanst, P.L., Wilson, W.E., Patterson, R.K., Gay, B.W., Jr., Chaney, L.W., and Burton, C.S., "A Spectroscopic Study of California Smog," EPA Report No. 650/4-75-006, Feb 1975.

9. Loper, G.L., "Air Oxidation of UDMH, Gas Phase Kinetics," CEEDO-TR-78-14, Paper No. 12, March 1978.

10. Pierson, R.H., Fletcher, A.N. and Gantz, E.S., "Catalog of Infrared Spectra for Qualitative Analysis of Gases," Analytical Chemistry, 28, 1218, (1956).

11. Pitts, J.N., Jr, Harris, G.W., Atkinson, R., Graham, R.A., and Winer, A.M., "Atmospheric Chemistry of Hydrazines: Gas Phase Kinetic and Mechanistic Studies," USAF Contract No. S0863-78-C-037, State-wide Air Pollution Research Center, University of California, Riverside CA 92521.

ADDITIONAL WORK ON HYDRAZINE OXIDATION

EXPLANATORY NOTE: Research completed and reported in CEEDO-TR-78-17 on hydrazine autoxidation in the long path cell was significantly extended due to major improvements in the long path cell. These updated experiments are presented in this section for comparison with similar studies on MMH.

EXPERIMENTAL

The preparation of a hydrazine calibration curve for the 0-10 ppm concentration range proved to be somewhat difficult. It was found that the technique of filling the double ended transfer bulb with hydrazine and flushing into the long path cell (as was done with MMH) gave consistently lower than expected results. Consistent results were finally obtained by injecting known quantities of hydrazine into the long path along with a 1.0-microliter syringe, then letting the sample sit for one hour to stabilize. By following this procedure, and plotting absorbance (at 958 cm^{-1}) versus the concentration (in ppm) times pathlength (in cm) product the extinction coefficient at 958 cm^{-1} was obtained as ln (10) times the slope of the line. This plot is shown in Figure A-1.

Hydrazine oxidation experiments in the long path cell were carried out in the same manner as the MMH oxidation experiments described in the body of this TR. However, 5.0 ppm methane was added with the hydrazine at the beginning of each run to monitor the path length.

RESULTS

Hydrazine decay in a synthetic atmosphere (20 percent O_2- 80 percent He) followed pseudo first order kinetics as can be seen from Figure A-2 where two different runs are plotted. The rate constant was 5.1 ± 0.1 x

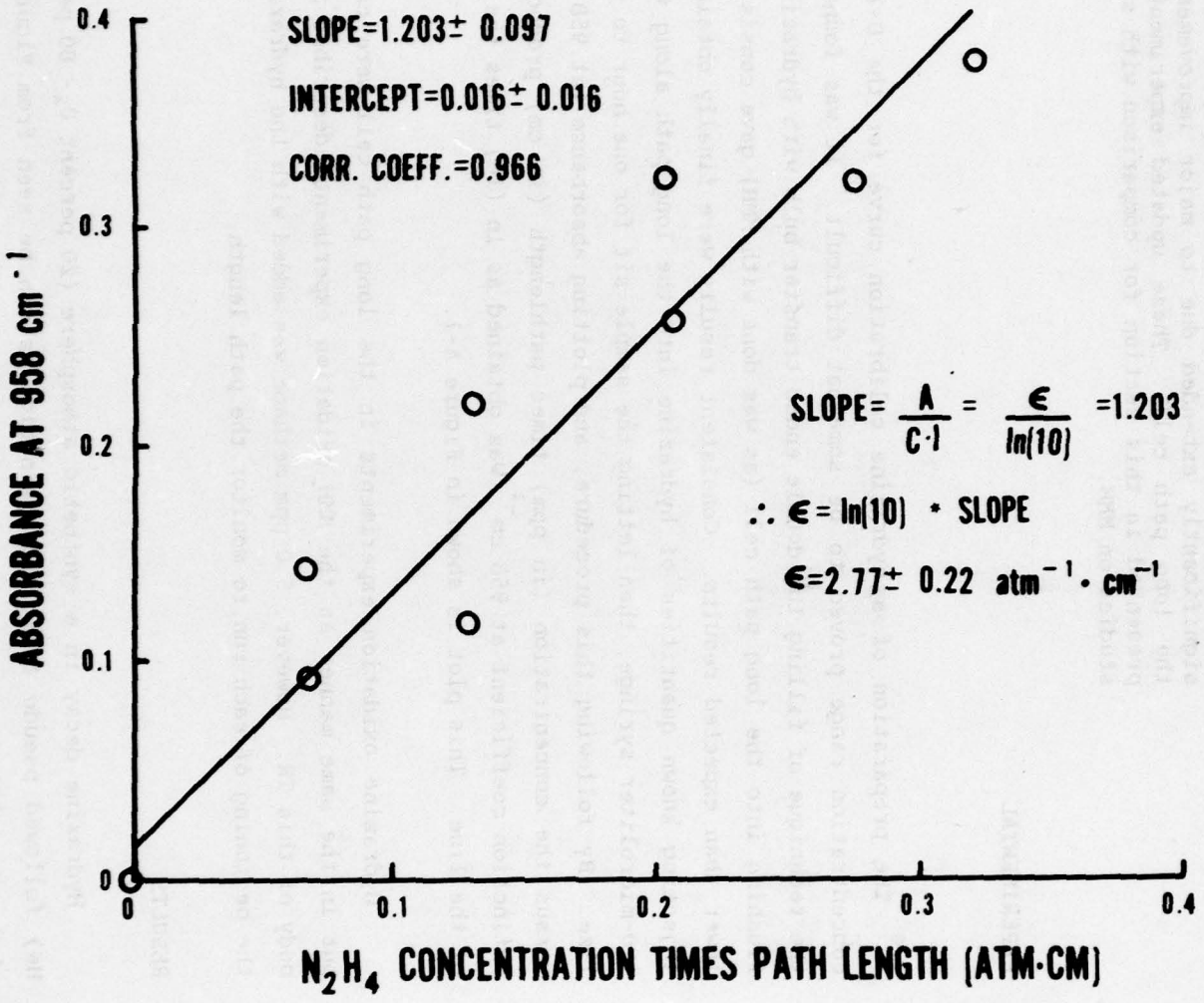

Figure A-1. Plot of Hydrazine Absorbance versue the Concentration - Path Length Product for Molar Extinction Coefficient Determination

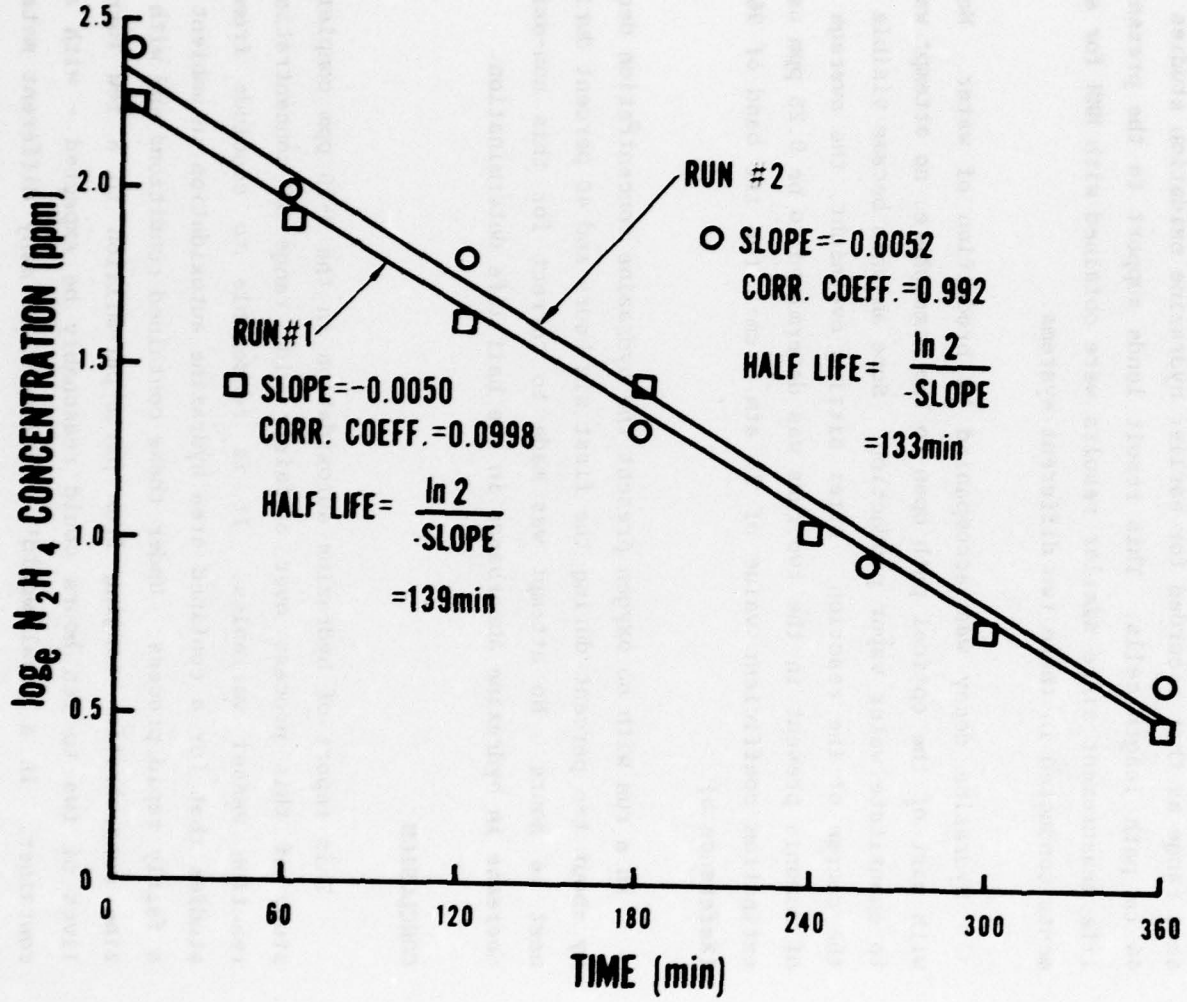

Figure A-2. Plot of Log_e Hydrazine Concentration versus Time Showing Pseudo First Order Behavior in Two Separate Experimental Runs

10^{-3} min^{-1}. The hydrazine half life under these conditions was about 135 minutes ($t_{\frac{1}{2}}$ = ln 2/k). This result is much shorter than earlier results described in Reference 3. The reason for this large difference is not known but must be tied closely to the differences in the ways the two experiments were carried out. The present half life measurement is in the same range as that recorded for earlier hydrazine oxidation studies in the 44 cm path length cells. This result lends support to the present half life measurement since similar results were obtained with MMH for experiments conducted in these two different systems.

Hydrazine decay was accompanied by production of water. However, with part of the optical path open to the atmosphere, no attempt was made to quantitate water vapor production. Some ammonia became visible during the course of the reaction. After sitting overnight, the average amount of ammonia present in the two runs was determined to be 0.25 ppm using an extinction coefficient value of 35 atm^{-1} cm^{-1} for the band of 966 cm^{-1} (Reference 8).

In a run with no oxygen present the hydrazine concentration decreased by about ten percent during the first six hours and 40 percent during the next 16 hours. No attempt was made to correct for this non-oxidative decrease in hydrazine absorbance in the half life determination.

CONCLUSION

This report of hydrazine autoxidation in the 0-10 ppm completes the study of this process over a fairly wide range of concentrations and reaction vessel variables. It is reasonable to conclude from these studies that for a confined area hydrazine autoxidation in ambient air is a fairly rapid process. Under these contained conditions and with hydrazine concentration ranging from parts-per-million to a few Torr, half lives of two to ten hours could reasonably be expected - with a glass container. In a 'real world' environment of many different metals and other surfaces present in a confined area, the autoxidation half life would surely be reduced somewhat, and probably a great deal due to catalytic enhancement of the oxidation process by these reactive surfaces.

INITIAL DISTRIBUTION

DDC/DDA	2	OEHL/CC	1
HQ AFSC/DL	1	HQ AFESC/DEV	1
HQ AFSC/SD	1	USAFSAM/EDE	2
HQ USAF/LEEV	1	HQ AFISC	2
HQ USAF/SGPA	1	HQ AUL/LSE 71-249	1
OSAF/MIQ	1	HQ USAFA/Library	1
OSAF/OI	1	HQ AFESC/TST	1
AFIT/Library	1	OL-AD; USAF OEHL	1
AFIT/DE	1	OUSDR&E	1
Federal Laboratory Program NSF	1	USAF Hospital, Wiesbaden	1
USAF Chief, R&D/EQ	1	USAFSAM/CC	1
EPA/ORD	1	AFOSR/CC	1
USN Chief, R&D/EQ	1	HQ AFSC/DEV	1
HQ MAC/DEEE	1	HQ TAC/DEEV	1
HQ ADCOM/DEEV	1	HQ SAC/DEPA	1
HQ AFLC/DEPV	1	HQ PACAF/SGPE	1
HQ AFESC/RDVC	15	HQ ADCOM/AGPAP	1
USAFRCE/WR	1	HQ ARC/SGPAP	1
USAFRCE/CR	1	HQ AAC/SGB	1
USAFRCE/ER	1	HQ AFLC/SGB	1
HQ USAFE/DEPV	1	22 CES/DE	1
HQ USAFE/DEVS	1	AMD/RDB	1
OASD (I&L)ES	1	AMRL/THE	1
HQ USAFE/SG	1	AFRES/DEEE	1
HQ AFSC/SGB	1	1 Med Service Wg/SGB	1
HQ TAC/SGPA	1	USA Environ Hygn Agency	1
HQ SAC/SGPA	1	Commander USA MB R&D Lab	1
HQ MAC/SGPE	1	Toxi Matls Info Center	1
SAALC/SFQT	1	Swiss Fed Institute of Tech	1
HQ USAF/SAFMIQ	1	Environmental Research Lab	1
HQ USAF/SAFOI	1	Syracuse Research Corp	1
		USAF Hospital/OEHL	1
OASD/(MRA&L) EES	1	USAFSAM/VNL	1
CINCAD/SGPAP	1	AFRPL/Library	1
NCEL, Code 25111	1	AFRPL/LKDP	1
Stanford University	1	HQ ASD/YPLL	1
Calif Inst of Technology	1	FTD/LGM	1
Mass Inst of Technolgoy	1	ADTC/DLODL	1
AMD/RDU	1	SAMSO/DEV	3
AMD/RDB	1	SAMSO/LV-1	1
6595 STESTG/SZ	1	SAMTEC/SEM	1
6595 STESTG/TS	1	OG-ALC/SGP	1
1 STRAD/SEM	1	ARPA	1
EPA PNERL	1	DD-MED-41	1
USAF Hospital/SGP	1	USAF Hospital/SGP	1
USAF/Hospital/SGP	1	USAF Hospital/SGP	1
SA/ALC/SFQ	1	USAFOEHL/EC	1
AFOSR/NL	1	Aberdeen Proving Ground	1

INITIAL DISTRIBUTION (Continued)

MIT Lincoln Lab	1	AFRPL/LKCP	1
SAMSO/SGX	1	USAF Hospital/SGPB	1
SDSAN-DQ-QS	1	Aerospace Corp	1
6570 AMRL/THE	1	USAFSAM/VNL	1
Eglin Reigonal Hospital	1	Chief USAEHA	1
USAF SAMSO/DEV	1	AFIT	1
HQ AFLC/SGB	1	Olin Corporation	1
US Army MIRADCOM	1	NASA/DL-DED-32	1
Florida Institute of Tech	1	Ohio State University	2
6585th Test Group (TKS)	1	Chemical Abstracts Service	1
SA-ALC/SFQT	1	Martin Marietta	1
NASA/MD-E	1	University of Calif	2
HQ AFESC/RDV	5	HQ AFESC/RDVW	5
KSC Library	1	OUSDR&E	1

HQ AFESC/RDXX
Tyndall AFB FL 32403

OFFICIAL BUSINESS

THIRD CLASS